IVYSPRING INTERNATIONAL PUBLISHER

International Journal of Biological Sciences

2024; 20(2): 765-783. doi: 10.7150/ijbs.91295

Review

Radiotherapy in Preclinical Models of Brain Metastases: A Review and Recommendations for Future Studies

Wen Shi[1#], Guilong Tanzhu[1#], Liu Chen[1], Jiaoyang Ning[1], Hongji Wang[1], Gang Xiao[1], Haiqin Peng[1], Di Jing[1], Huadong Liang[2], Jing Nie[2], Min Yi[2], Rongrong Zhou[1,3,4]✉

1. Department of Oncology, Xiangya Hospital, Central South University, Changsha, 410008, Hunan Province, China.
2. Department of Technology, Hunan SJA Laboratory Animal Co., Ltd., Changsha, Hunan Province, China.
3. Xiangya Lung Cancer Center, Xiangya Hospital, Central South University, Changsha, 410008, Hunan Province, China.
4. National Clinical Research Center for Geriatric Disorders, Xiangya Hospital, Central South University, Changsha, 410008, Hunan Province, China.

# Wen Shi and Guilong Tanzhu contributed equally to this work.

✉ Corresponding author: Rongrong Zhou, Department of Oncology, Xiangya Hospital, Central South University, No. 87 Xiangya Road, Kaifu District, Changsha, 410008, China, E-mail: zhourr@csu.edu.cn.

Received: 2023.10.19; Accepted: 2023.12.14; Published: 2024.01.01

Abstract

Brain metastases (BMs) frequently occur in primary tumors such as lung cancer, breast cancer, and melanoma, and are associated with notably short natural survival. In addition to surgical interventions, chemotherapy, targeted therapy, and immunotherapy, radiotherapy (RT) is a crucial treatment for BM and encompasses whole-brain radiotherapy (WBRT) and stereotactic radiosurgery (SRS). Validating the efficacy and safety of treatment regimens through preclinical models is imperative for successful translation to clinical application. This not only advances fundamental research but also forms the theoretical foundation for clinical study. This review, grounded in animal models of brain metastases (AM-BM), explores the theoretical underpinnings and practical applications of radiotherapy in combination with chemotherapy, targeted therapy, immunotherapy, and emerging technologies such as nanomaterials and oxygen-containing microbubbles. Initially, we provided a concise overview of the establishment of AM-BMs. Subsequently, we summarize key RT parameters (RT mode, dose, fraction, dose rate) and their corresponding effects in AM-BMs. Finally, we present a comprehensive analysis of the current research status and future directions for combination therapy based on RT. In summary, there is presently no standardized regimen for AM-BM treatment involving RT. Further research is essential to deepen our understanding of the relationships between various parameters and their respective effects.

Keywords: Brain metastasis; Radiotherapy; Dose fractionation, Radiation; Animal models; Combined modality therapy

Introduction

With prolonged patient survival and advancements in imaging technology, the incidence of brain metastases (BMs) is on the rise [1-4]. Common primary tumors associated with BM include lung cancer [5-7], breast cancer [4,8,9], and malignant melanoma [10, 11]. Despite multiple interventions, such as surgery, radiotherapy (RT), and chemotherapy, patients with brain metastases face disappointingly short survival, with a 2-year survival rate that is less than 10% [12]. In recent years, the application of targeted therapy and immunotherapy has led to improvements in survival [4,12,13].

Radiotherapy (RT) is the cornerstone treatment for BM and enhances the local control rate [14] and reduces BM recurrence [15-18]. The RT options for BM treatment include whole-brain radiotherapy (WBRT) [19] and stereotactic radiosurgery (SRS) [20-22]. Prophylactic cranial irradiation (PCI), a unique form of RT, is known to delay and reduce the occurrence of BM [23-25]. WBRT is typically recommended for patients with multiple brain metastases (usually > 3 lesions [19]), while SRS may serve as the standard treatment for oligometastatic lesions (usually ≤ 4 lesions [20-22, 26]). In addition to its direct impact on the BM, RT alters the tumor microenvironment and the permeability of the blood-brain barrier (BBB), laying

the foundation for combination therapies [27-29]. Currently, the sequence and timing of combining RT with immunotherapy [30-34], targeted therapy, or new treatments such as nanomaterials [35-38] are key research areas in the field of BM treatment.

Animal experiments play a pivotal role in preclinical research, offering a theoretical basis for clinical translation. However, distinct treatment regimens yield varied effects, and the parameters from model establishment to treatment delivery are diverse. Although RT parameters (such as RT mode, dose, dose rate, fractionation, etc.) have been explored in subcutaneous models of various tumors, these models are limited by replicating the intrinsic structure of the BBB and the unique immune microenvironment of the BM. Consequently, honest evaluations of RT and drug efficacy for treating BM are challenging. Intracranial patient-derived tumor xenograft (PDX) models, more akin to the phenotype and genotype of BM patients than subcutaneous PDX models [39,40], are crucial for assessing local curative effects and their mechanisms [13].

Currently, RT parameters in animal models of brain metastases (AM-BMs) lack standardization, and there is a dearth of reviews on this topic. This review, based on AM-BM, systematically summarizes RT regimens for BM for the first time, covering model establishment for RT implementation, and providing a reliable foundation for subsequent research. Additionally, comprehensive treatment is the primary approach for treating BM. We consolidate the schemes and molecular mechanisms of RT combined with other treatments.

Establishment of AM-BM and the Intervention Time of RT

Various methods are employed for the establishment of AM-BMs including intracerebral [33,39,41-50], intracardiac [31,32,51-54], carotid artery [55] and tail vein injection [56,57]. Few studies have explored spontaneous [58] or induced AM-BM [58,59]. Mice are the most commonly used animals for AM-BM [30,38,41,43,49,56,60-65]. The growth and therapeutic effects of AM-BM were monitored using *in vivo* imaging systems (IVIS) or magnetic resonance imaging (MRI), despite the relatively small volume of the BM (**Figure 2E**). The evaluation indicators for RT efficacy in AM-BM typically include tumor size and lesion size, overall survival, Ki67, Caspase-3, γH2AX expression, and so on (**Figure 2G**).

Establishing brain-tropic cells (brain metastasis cells) requires *in vivo* and *in vitro* screening. The selection process involves modifying cancer cells with reporter genes such as luciferase or GFP, which allows changes to be easily visualized, assessed, and prepared, using IVIS or MRI. Additional rounds of selection are then carried out. The modified cells are then reintroduced into the mice, usually after a period of growth outside the body (**Figure 1**).

The methods for establishing AM-BMs are multifaceted, each with pros and cons. Intracerebral injection (mostly in the striatum [33,39,41-48] or cerebral cortex [49]) can swiftly cause the formation of a single lesion [36], leading to high success rates. This method effectively summarizes BM growth and proliferation [66,67]. However, this approach disrupts the BBB, neglects the metastasis and colonization process, and thereby weakens predictive accuracy of treatment efficacy [59]. Arterial inoculation (internal carotid artery and intracardiac injection) is complex [68] and has low success rate [69,70]. Due to hematogenous metastasis, the location or lesions of intracranial tumors are randomized, and the formation of multiple extracranial metastases is unavoidable [71]. Intravenous (IV) inoculation (tail vein injection) is uncommon due to the low incidence of BM formation and inevitable lung metastases. Spontaneous models frequently form a single lesion in the BM [58], reflecting the actual process from tumor occurrence to metastasis. However, extensive use is hindered by the prolonged experimental period and metastases throughout the body [68]. Given these considerations, we highlighted precautions for model construction and detection indicators in the AM-BM (**Figure 2**).

The chosen modeling method influences the RT mode (**Figure 3B**). For intracerebral inoculation modeling, SRS [42,72,73] or WBRT [30,33,37,38,45,46,49,74,75] were commonly applied. Arterial inoculation-constructed AM-BM often involves WBRT [31, 32, 51-55]. Additionally, PCI is used for AM-BMs established through intravenous (IV) inoculation via tail vein injection [56,57]. Different model-building parameters and growth characteristics of BMs led to variable RT implementation times (**Figure 3B**).

The irradiation time of AM-BMs varies based on the inoculation methods (intracerebral earlier than systemic) and animal species (mouse earlier than rats) [48]. In syngeneic models, BMs proliferate faster than in xenograft models, suggesting a shorter treatment window [68]. For intracerebral injection of lung/breast cancer AM-BM, irradiation time is closely tied to injection cell number, generally, beginning within 2 weeks for 10^6 cells [46,76] and within 2-3 weeks for 10^4 cells [45,75,77]. In melanoma AM-BM, irradiation of 10^2-10^4 cells usually occurs within 1-2 weeks [33,34,42,48,73]. In particular, PCI is administered within one week of cell inoculation [56,57,78]. The relationship between the implanted cell counts and RT intervention time is shown in **Table 1**.

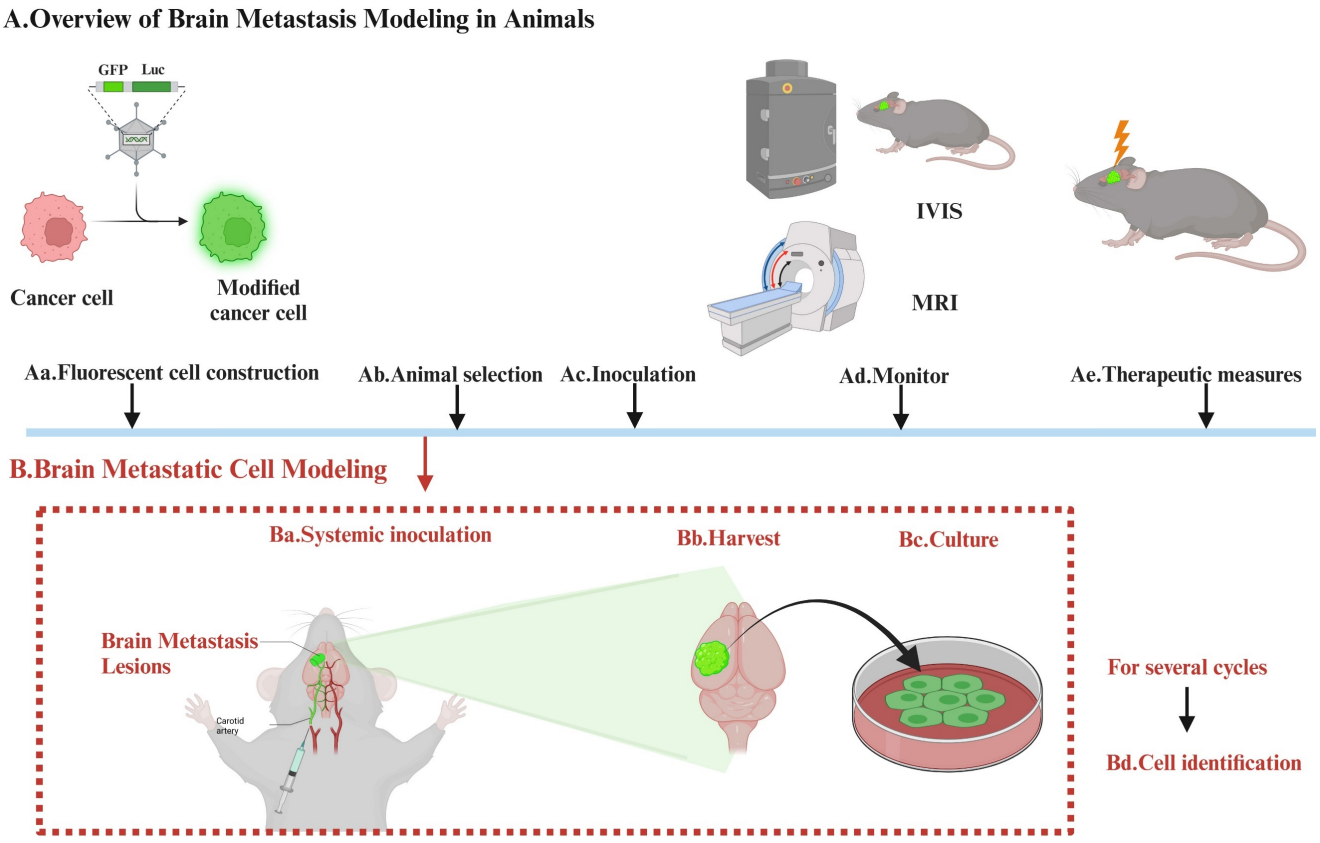

Figure 1. The Process of Establishing Brain Tropic Cells. Establishing brain-tropic cells (brain metastasis cells) requires *in vivo* and *in vitro* screening. The selection process involves modifying cancer cells with reporter genes such as luciferase or GFP, which allows changes to be easily visualized, assessed, and prepared, using IVIS or MRI. Additional rounds of selection are then carried out. The modified cells are then reintroduced into the mice, usually after a period of growth outside the body.

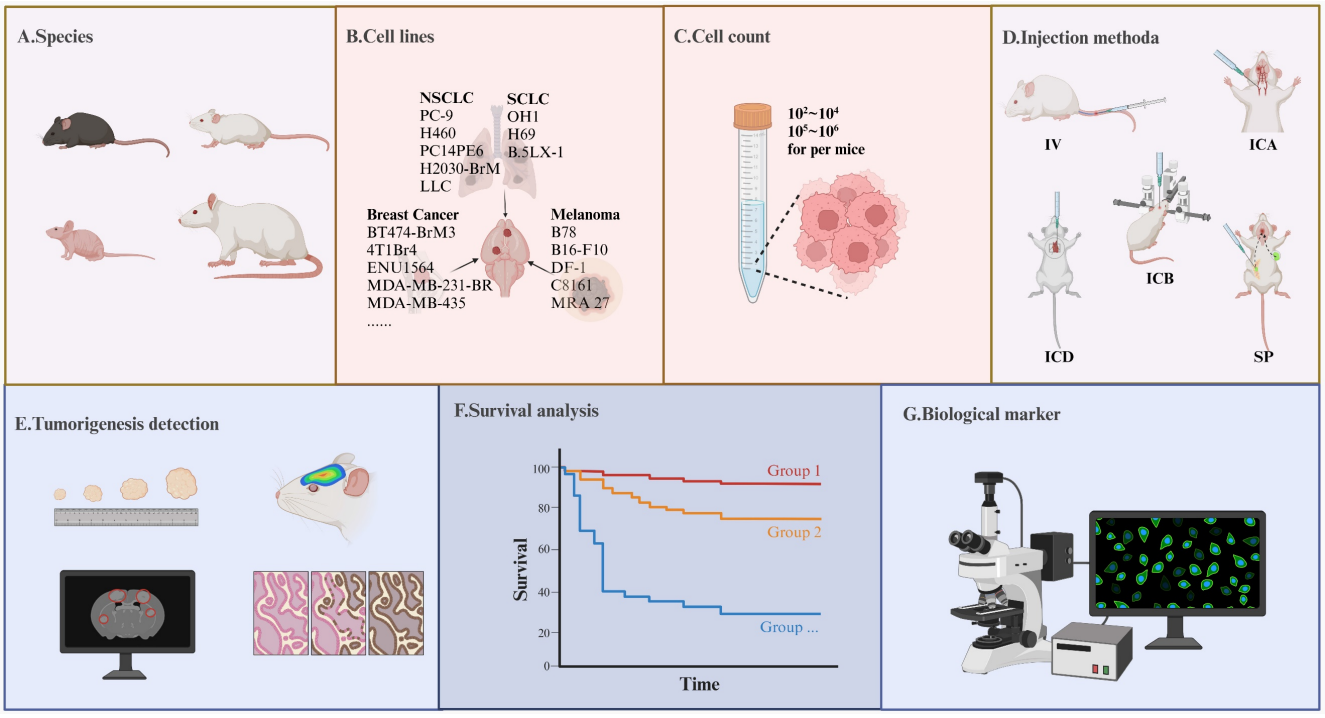

Figure 2. Precautions in Model Construction and Detection Indicators in the AM-BM. (A-D) Several key parameters significantly influence the tumor formation rate during AM-BM model development. (A) Species including C57BL/6 mice, SCID mice, BALB/c nude mice, and rats are frequently utilized in AM-BM studies. (B) Various cell lines, such as lung cancer (H2030-BrM, PC-9-BrM3), breast cancer (BT474-BrM3, 4T1Br4), and melanoma cell lines (B16-F10, B78), are commonly employed for AM-BM establishment. (C) The quantity of injected cells is a critical determinant of successful model construction and the optimal time window for treatment. (D) Current BM modeling methods encompass intracerebral injection (ICB), intracardiac injection (ICD), internal carotid artery injection (ICA), tail vein injection (IV), and spontaneous or induced models (SP). (E-G) Common parameters assessed in in-vivo studies include: (E) Tumor lesion, tumor number, and tumor volume. (F) Survival. (G) Tumor biomarkers, such as the expression of Ki67, γH2AX, and so on.

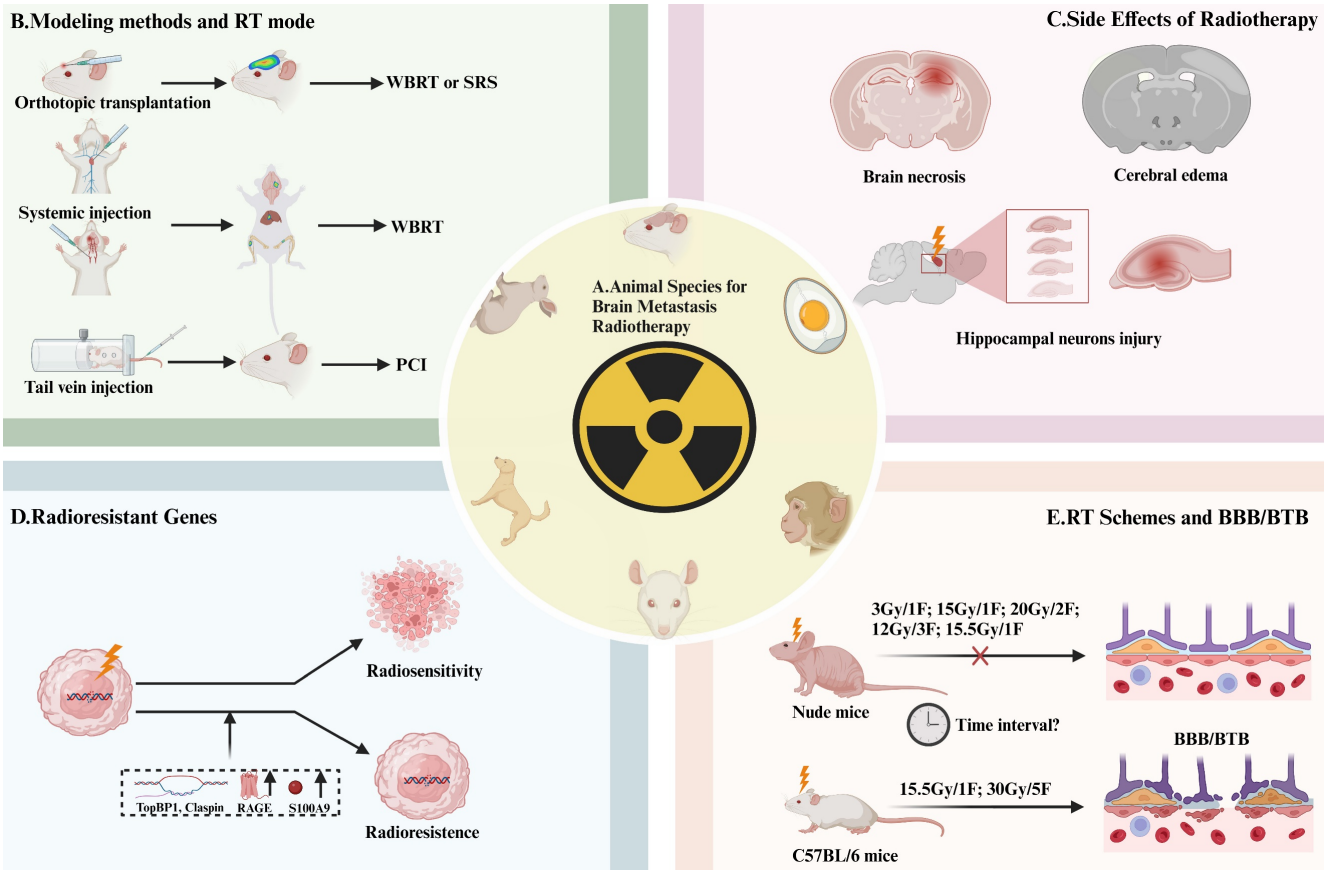

Figure 3. Animal Species, Irradiation Methods Selection, and Effects of RT on AM-BM. (A) Animal species currently employed in RT studies of AM-BM encompass mice, chicken embryos, monkeys, rats, dogs, and rabbits. (B) Different irradiation methods are utilized based on the modeling approach: SRS or WBRT is commonly applied for local inoculation modeling, WBRT for intracardiac and internal carotid artery injections, and PCI for tail vein injection. (C-D) The prognostic factors influencing survival were as follows: (C) RT-induced side effects on brain tissue, such as radiation edema, necrosis, neurotoxicity, and hippocampal damage. (D) Factors such as radiation resistance genes (TopBP1 and Claspin), secretion of S100A9, and the overexpression of RAGE limit the survival benefits of RT. (E) *In vivo* studies reveal differential responses of the blood-brain barrier/blood-tumor barrier in various mouse strains to RT. Notably, doses of 3 Gy/1F, 12 Gy/3F, 15 Gy/1F, 15.5 Gy/1F, and or 20 Gy/2F did not significantly alter the permeability of the blood-brain barrier/blood-tumor barrier in BALB/c nude mice. However, doses of 15.5 Gy/1F and 30 Gy/5F can induce changes in the blood-brain barrier/blood-tumor barrier permeability in C57BL/6 mice. The time window during which RT induces BBB/BTB opening in AM-BMs has not been determined.

Dose and Fractionation of RT in AM-BM

RT is a conventional therapy for BM [17]. However, the diversity of RT regimens in AM-BM across multiple studies underscores the necessity for standardization. Currently, WBRT is widely applied in AM-BM [30,33,34,37,38,45,46,49,54,74-77,79], followed by SRS [42,72,73]. Various parameters influence RT efficacy, including the RT method, dose, fractionation, dose rate, and intervention time. A comprehensive summary of these parameters was obtained from available radiotherapy studies in AM-BM (**Table 2-6**). Additionally, a comprehensive and scientific template for reporting experiments involving AM-BM and RT is shown in **Table 7**.

The linear-quadratic (L-Q) model, typically used to calculate the biologically effective dose (BED) of different fractionation schemes employs the formula $BED = D [1 + d/(\alpha/\beta)]$ [80]. The alpha/beta ratio(α/β), total dose (D), and fractional dose (d) are integral components [81]. The criteria for RT schemes in AM-BM include (1) clinical regimens [62,74,76], (2) BED equivalent schemes [33,34,38,45,54,75,76,79], (3) previous experience based on different research objects [35-37,50,52,56], and (4) protection of normal tissues [49,55,82]. The first two criteria are generally applied.

WBRT

WBRT is widely employed in AM-BMs. The 30 Gy/10F or 20 Gy/5F regimens [83] are recommended by the National Comprehensive Cancer Network (NCCN) guidelines for BM patients [84], while preclinical studies typically administer WBRT at a total dose ranging from 15 Gy to 20 Gy in a single or fractionated high-dose irradiation format [33,34,38,45,54,75,76,79].

As indicated by previous reports, lower doses (< 15 Gy) of WBRT have been explored due to their ability to inhibit tumors and prolong survival [36,37,52,56]. Notably, a study implementing WBRT (12 Gy/3F) significantly restricted tumor volume but failed to reduce the number of BM lesions [52]. In AM-BM of breast cancer, Choi et al. demonstrated that 10 Gy/1F exhibited a stronger inhibitory effect

than 5 Gy/1F, with no significant difference observed with 20 Gy/1F [65]. Compared with those treated with 5 Gy/1F, 15 Gy/1F, or 20 Gy/1F, animals treated with BM via the 10 Gy/1F regimen had the longest survival [50]. In combination therapy, the use of WBRT (7 Gy/1F) with nanoparticles for AM-BM of melanoma demonstrated a reduced RT dose and prolonged survival [36].

Using the L-Q model, the BED of RT regimens (15-16 Gy/1F, 20 Gy/2F) in AM-BM was found to be comparable to the clinical regimens of 30 Gy/10F, assuming the α/β value of 10 [54,76,78,79]. Zarghami et al. and Murrell et al. employed 16 Gy/1F and 20 Gy/2F, respectively, and showed significant reductions in BM lesions and tumor volume [54, 79]. Due to the limited access to synchrotron radiation sources, some studies have applied single-dose fraction RT [85], which saves time but may increase the risk of edema and necrosis.

To mitigate side effects, certain studies have adopted regimens with lower BED for normal tissue [49,55,82]. Martínez-Aranda et al. demonstrated that the 16.5 Gy/3F protocol [55], which involves a BED lower than 30 Gy/10F, significantly alleviated brain toxicity and reduced the frequency of intraperitoneal anesthesia, partially circumventing accidental death [55]. Similarly, Prociss et al. verified that the 10 Gy/5F regimen effectively avoided neurotoxicity in AM-BM [49]. To overcome radiation resistance in melanoma and prevent radiation necrosis simultaneously, Wall et al. raised the single dose to evaluate the effect of RT (12 Gy/3F) [82].

Alterations in the tumor microenvironment following radiation exposure also led to varied effects on tumor eradication. Different RT fractions with equivalent doses led to diverse responses of immune cells [31,32]. Schulz et al. reported that compared with that of 10 Gy/1F, 10 Gy/5F increased monocyte-derived macrophage (TAM-MDM) infiltration. However, the former regimens reduced TAM-MDMs and, more significantly, altered the expression of genes related to pro-inflammatory host defense responses in peripheral myeloid cells [32]. Distinct RT fractions with the same BED generated diverse inhibitory effects. For instance, 30 Gy/10F significantly reduced intracranial metastases, while 15 Gy/1F was more beneficial for median survival [76].

Table 1. Cells Account and RT Intervention Schedule for Intracerebral Injection (Part 1) and Other Injections (Part 2) (including internal carotid artery and intracardiac injection).

Part 1			
Cancer type and cell count	**0-1 Weeks**	**1-2 Weeks**	**2-3 Weeks**
Lung cancer			
10^3-10^4	NA	1×10^4 (WBRT, PC14PE6) [45, 75]	NA
10^4-10^5	NA	1×10^5 (WBRT, LX-1) [77]	1×10^5 (WBRT, LLC) [71]
10^5-10^6	2×10^5 (WBRT, PD*) [46]	NA	1×10^6(conformal RT, H460) [43]
Breast cancer			
10^3-10^4	5×10^3 (SRS, MADB106) [72]	NA	1×10^3 (IMRT, ENU1564) [112]
10^4-10^5	2×10^4(WBRT, MDA-231-Br) [37]; 2.5×10^4(WBRT, E0771-BrM3) [88]	NA	1×10^5 (WBRT, MDA-MB-435) [44]
10^5-10^6	NA	1×10^6 (WBRT, MDA-231-Br) [76]; 4×10^5 (WBRT, BT474-Br-M3) [77]	1.75×10^5 (WBRT, MDA-231-Br) [87]
Melanoma			
10^2-10^3	3×10^2 (SRS, B16-F10) [73]; 5×10^2 (SRS, B16-F10) [42]	NA	NA
10^3-10^4	NA	2×10^3 (WBRT, B16) [33]; 5×10^3 (WBRT, B16-F10) [34]	NA
10^5-10^6	NA	1×10^6 (IR*, MRA 27) [48]	NA
Ehrlich ascites tumor			
10^5-10^6	1.5×10^5 (WBRT, Ehrlich ascites tumor cells) [50]	NA	NA
Part 2			
Cancer type and cell count	**0-1 Weeks**	**2-3 Weeks**	**3-4 Weeks**
Lung cancer			
10^5-10^6 cells	1×10^5 (WBRT, H2030-BrM; intracardiac injection) [88]	2×10^5 (WBRT, LLC; intracarotid artery) [71]	NA
Breast cancer			
10^4-10^5 cells	NA	3×10^4 (WBRT, TS1-BrM; intracardiac injection) [31]; 1×10^5 (WBRT, 99LN-BrM; intracardiac injection) [31]	NA
10^5-10^6 cells	1.75×10^5 (PCI, MDA-231-Br-HER2; intracardiac injection) [78] 5×10^5 (PCI, MDA-IBC-3; tail vein injection) [56]	1.75×10^5 (WBRT, C8161; intracardiac injection) [76]; 2×10^5 (WBRT, MDA-231-Br; intracardiac injection) [52];	1×10^5 (WBRT, MDA-231-Br; intracardiac injection) [54]; 1.5×10^5 (half brain radiation, MDA-231-Br; intracardiac injection) [79]; 1×10^6 (WBRT, 435-Br1; intracarotid artery) [55]

*PD: patient-derived tissue cells; IR: No specific radiotherapy method was mentioned.

Table 2. Relevant Parameters of Radiotherapy Research in the AM-BM (WBRT combined CTR, IT, TT, etc.)

Cancer	Species	Monitoring intracranial tumor formation	Injection method	Injection site	Cell line	Cell number/ volume (cells/μl)	Irradiator	Irradiation time (days)	Dose/ fraction (Gy/F)	Dose rate (Gy/ min)	Combination therapy	Effect	Ref
NSCLC	8w Male athymic nude mice	NA	ICB	Left striatum	PC14PE6 (used modeling) H23	$1\times10^4/5$	IBL 437C blood Irradiator	14	15/1	2.3	TT: Chk1 AZD7762	Median Survival RT ↑ RT+AZD7762 ↑↑	[45]
NSCLC	Female nude (rnu/rnu) rats	Fluorescent oligonucleotide delivery	ICB	Right caudate nucleus	H460	$1\times10^6/10$	RadSource RS2000 Irradiator Versa HD (Elekta, Stockholm, Sweden) linear accelerator	21 (D283) 5 (H460)	2/1 (athymic rat) 5/1 (normal Long Evan rats)	NA	CTR+TT: TMZ (20 mg/kg × 4 days) anti-MGMT morpholino oligonucleotides (AMONs) (10.5 mg/kg; IV) (1 d after radiation)	(vs. RT+TMZ) Tumor volume RT+TMZ+AMON ↓ (RT+AMON vs RT) MGMT — BCL-XL — p27 —	[43]
NSCLC	7-8w BALB/c nude mice	Detecting fluorescence intensity.	ICD	NA	PC-9 (modeling) H3255	NA/100	XCELL 160 X-ray system (Kubtec, Stratford, CT, USA)	intracranial fluorescent signal $>5\times10^6$ photons /s (1-3W)	30/10	1.6	TT: EGFR AZD3759 or osimertinib (1 h prior to the RT)	Tumor volumes RT ↓ RT + AZD3759 ↓↓↓ RT + osimertinib ↓↓	[62]
NSCLC	6-8w Female nu/nu mice	Bioluminescence signals	ICB	Brain parenchyma	PC-9 (modeling) H3255 H2228 H226	5×10^5/NA	XCELL 160 X-ray system	NA	30/10 15/1 3/1	1.6	TT: EGFR 1 h before radiation. (AZD3759 was administered by oral gavage at 15 mg/kg once daily until the end of the study)	*In vivo* (vs RT) Tumor volume RT+AZD3759↓↓ Ki-67 RT↑ (3h) — (8h) RT+AZD3759↓↓ CC3 RT↑ RT+AZD3759↑↑	[74]
NSCLC	6-8w Female athymic Nude-Foxn1nu mice	IVIS	ICB	Right striatum	PDX*	$2\times10^5/5$	Xstrahl Small Animal Radiation Research Platform (SARRP)	3	12.5/5	2.68	TT: ATR M6620(60 mg/kg by daily oral gavage)	M6620 treatment combined with radiotherapy synergistically and successfully inhibits cancer growth (PDX)	[46]
NSCLC	6-8w Female C57BL mice	IVIS 1. 14 days 2. 6 days	1. ICA 2. ICB	Right striatum	LLC	1. $2\times10^5/100$ 2. $1\times10^5/5$	Varian Clinac 600C X-ray unit	1.21 2.13	10/1	2.5	TT: CXCR4 Endostar (ES) (Treatment 14 days after IVIS imaging)	*In vivo* Tumor size RT↓ RT + Endostar↓↓ The vessels: RT + Endostar more regular and pericyte	[71]
Melanoma	6-7w athymic nude mice	IVIS	ICB	0.5 mm anterior and 2 mm lateral to the bregma	C8161	$1\times10^4/5$ (0.6 μL /min)	γ-irradiator (Gammator 50, cesium 137 source)	NA	16/4/4 weeks	NA	TT: GRM1 Riluzole	Tumor volume RT ↓ RT + Riluzole ↓↓	[82]
Melanoma	6-8w Female C57BL/6 mice	NA	ICB	Right striatum	B78	2×10^5/NA	X-RAD 320 (Precision X-Ray Inc., North Branford, CT)	Day 1 after flank irradiation or day 15	4/1	NA	IT: ISV (1 day) + anti-CTLA-4(3,6,9 days)	Relatively low-dose WBRT (4 Gy) or targeted radionuclide therapy increases the number of T lymphocytes (CD4+ and CD8+) and monocytes/macrophages (F4/80+) and improves immunotherapy of bone marrow melanoma reaction.	[30]
Melanoma	6w C57BL/6J mice	MRI	ICB	NA	B16-F10	5×10^4/NA	320 kV X-ray generator	NA	7/1	2	AGuIX® (Gd-based nanoparticles) (10 mg, i.v.) (radiation 3.5 hours after injection)	*In vitro*: γ-H2A RT ↑ RT + AGuIX® ↑↑ *In vivo* Survival RT ↑ RT + AGuIX® ↑↑	[36]
Melanoma	C57BL/6 mice	IVIS	ICB	Left striatum	B16	200 untreated + 1,800 disabled [pre-irradiated by 100 Gy (several hours before implantation) /1 culture medium	Philips RT100 X-ray	8	15/1	7.6	IT: tumor vaccine granulocyte-macrophage colony-stimulating factor	Median Survival RT↑ RT + IT ↑↑ Tumor volume RT ↓ RT + IT ↓↓	[33]

Cancer	Species	Monitoring intracranial tumor formation	Injection method	Injection site	Cell line	Cell number/ volume (cells/μl)	Irradiator	Irradiation time (days)	Dose/ fraction (Gy/F)	Dose rate (Gy/ min)	Combination therapy	Effect	Ref
Melanoma	C57BL/6 mice	IVIS	ICB	Left striatum	B16-F10-luc2	250 B16-F10-luc2 + 5000 disabled B16 (100 Gy)/1 culture medium	Philips RT100 X-ray	8	15/1 18.75/1 22.5/1	7.6	IT	Median Survival 15 Gy ↑ 15 Gy + IT ↑↑ 18.75 Gy ↑ 18.75 Gy + IT ↑↑ 22.5 Gy ↑↑↑ 22.5 Gy + IT ↑↑↑	[34]
Ehrlich Ascites tumor	Female B6D2F1 mice	NA	ICB	Temporal hemisphere	Ehrlich ascites tumor (EHR2)	1.5×10^5/30	Stabilipan (Siemens, Munich, Germany)	3	10/1	4.7	CTR: etoposide + dexrazoxane	Median Survival (vs RT) 34 mg/kg etoposide + 125 mg/kg dexrazoxane + RT ↑ 90 mg/kg etoposide + 125 mg/kg dexrazoxane + RT ↑↑	[50]
Breast Cancer	6-8w Female athymic nude mice	PET/CT 3D MRI	ICB	Right frontal lobe	BT474-Br-M3	4×10^5/NA	Gamma Cell irradiator	8	10/ 5	NA	TT: Her2 Single-domain antibody fragments	synergistic effect	[49]
Breast Cancer	Athymic nude mice	IVIS	ICB	Left hemisphere	MDA-MB-231	1×10^5/1	Philips RT100 X-ray generator (Amsterdam, The Netherlands) operating at 100 kVp with a 1.7 mm Al filter.	NA	15/1	NA	Nano: INP (iodine nanoparticles) i.v. (1 d before radiation)	Median Survival RT ↑ INP + RT ↑ Tumor size RT ↓ INP + RT ↓↓	[38]
Breast Cancer	6w Female BALB/c nude mice	IVIS	ICB	Right striatum	MDA-231-Br	2×10^4/2	ELEKTA Irradiator (Precision X-Ray, UK)	5、17	10/2	NA	Leucine-rich repeat-containing protein 31 (LRRC31)	LRRC31 is a major DNA repair suppressor that can be targeted for cancer radiosensitization therapy.	[37]
Breast Cancer	6w Female athymic nude mice	NA	ICB	Left striatum	MDA-MB-435	1×10^5/5	IBL 437C blood Irradiator	15	10/1	2.3	TT: c-Met tyrosine kinase inhibitor	Survival RT ↑ RT + inhibit c-Met ↑↑ Tumor volume RT ↓ RT + inhibit c-Met ↓↓ apoptosis RT ↑ RT +c-Met depletion ↑↑	[44]
Breast Cancer	Female athymic nude-Foxn1nu mice	MRI	ICA	NA	MDA-MB-435-Br1	1×10^6/100	NA	27	16.5/3	240 Monitor Units (MU/ min)	CTR: Temozolomide	*In vivo* Survival RT + TMZ↑ vs. RT weight athymic mice—NOD/SCID mice ↓↓	[55]
Breast Cancer	12 w C57BL/6J 8w FVB/n mice	MRI	ICD	NA	99LN-BrM2 TS1-BrM	6×10^4 99LN-BrM 1×10^5 99LN-BrM 3×10^4 TS1-BrM	SARRP	(About 3W) MRI indicates the brain metastases	10/5	5.2 cGy/s	IT: anti-PD-1	the combination of WBRT with Anti PD-1 has been demonstrated to exert a synergistic anti-tumor effect.	[31]
Breast Cancer	R2G2 SCID mice	bioluminescence imaging (BLI)	1. ICB 2. ICD	1. Brain at a depth of 4 mm.	SKBrM3 231-BrM	1.SKBrM3: 2×10^4/5 231-BrM: 2×10^4/5 2. SKBrM3: 1×10^5 231-BrM: 2×10^5	X-Ray XRAD 320 Orthovoltage X-ray Unit with custom-made collimators (<5 mm diameter)	28 (When BLI reached 1×10^6)	40/4	NA	A thermal radiofrequency electromagnetic field (1 day after tumor implantation.)	Survival: RT ↑ RT + BCF ↑↑	[111]
Breast Cancer	8-12w 1.NOD-SCID IL2Rγnull (NSG) Female mice 2.Female C57BL/ 6 mice	IVIS	ICD	NA	1.JmT1BR3-GFP-luciferase 2.E0711-GFP-Luciferase	$1.2.5\times10^5$ 2.5×10^4	Precision X-Ray X-Rad 225Cx Micro IGRT and SmART Systems	7	1. 10/1 2. 35/1 10/1	4.8-5.8	Topiramate	Radiation-induced brain edema may be reduced by blocking AQP4	[127]

RT was found to delay the progression of BM and prolong survival in various studies [33,36,38,45,55,76,77,86]. Hofland et al. demonstrated that in AM-BM of Ehrlich's ascites cancer, RT significantly prolonged survival, with the 10 Gy/1F regimen showing more apparent effects [50]. In AM-BM of breast cancer, RT may achieve long-term survival [76]. However, individual studies reported conflicting conclusions [44,49,75,87]. For instance, Chae et al. showed that WBRT (10 Gy/1F) reduced tumor volume but had no significant effect on survival [53]. Similarly, regimens such as 30 Gy/10F, 16.5 Gy/3F, and 9 Gy/3F did not improve tumor progression and survival due to radiation resistance [88].

Reasons for Conflicting Results in WBRT Research in AM-BM:

(1) Impact of Model Establishment on Survival. Some studies suggest that the mode of model establishment may influence survival. Arterial inoculation, which can lead to widespread tumor metastasis, raises the concern that animal death may not be solely attributed to BM [76].

(2) Side Effects Caused by RT. The side effects of RT such as radiation edema, necrosis, nerve damage, and hippocampal damage can vary and impact study outcomes. WBRT (10-15 Gy) has been observed to inhibit nerve growth by inducing DNA double-strand breaks (DSBs) and apoptosis [53,76,89]. Additionally, single high-dose RT may lead to hippocampal toxicity [76,90] (**Figure 3C**).

(3) Inconsistent Radiosensitivity among Various Cancer and Cell Subtypes. The calculation of the biologically effective dose (BED) by the linear-quadratic (L-Q) model may be inaccurate, especially after standardizing the empirical rule $\alpha/\beta=10$ across various tumors [91]. Moreover, the L-Q model is not suitable for relatively high doses (>13 Gy) [92].

(4) Radiation-Resistant Genes. The presence of radiation-resistant genes, such as TopBP1, Claspin, and Caveolin 1, in AM-BM of NSCLC, may influence the effectiveness of RT (**Figure 3D**). These genes alleviate inhibition, leading to improved survival following RT [75,93]. Furthermore, the expression and secretion of S100A9 from BM cells, which binds to the RT-induced RAGE receptor, activate NF-κB mediated RT resistance [88] (**Figure 4K**).

In conclusion, these factors highlight the complexity of interpreting and comparing results across different studies. A summary of the relevant parameters for WBRT in AM-BM is provided in **Table 2 and Table 3**.

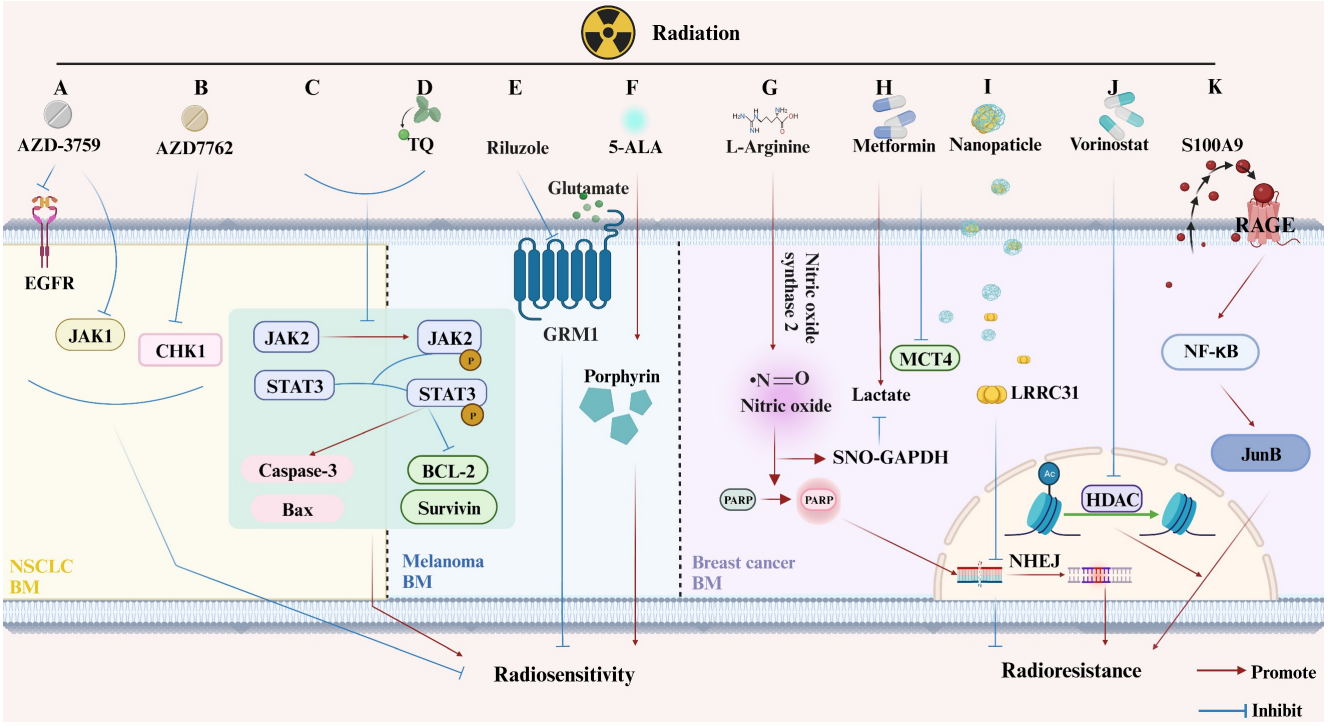

Figure 4. Changes in Molecular Pathway Induced by RT with or without Additional Treatments in Animal Models of Brain Metastases from Lung Cancer, Melanoma, and Breast Cancer. (A-C) Lung Cancer BM. (A) AZD-3759 enhances NSCLC radiosensitivity by inhibiting EGFR and JAK1; (B) AZD7762 promotes NSCLC radiosensitivity by suppressing CHK1; (C) RT inhibits phosphorylation of JAK2 and STAT3, inducing apoptosis. (D-F) Melanoma BM. (D) Thymoquinone (TQ) increases radiation-induced apoptosis by inhibiting JAK2 phosphorylation; (E) Riluzole enhances radiosensitivity of melanoma BM cells by inhabiting GRM1; (F) 5-ALA increases melanoma BM radiosensitivity by increasing the porphyrin content. (G-K) Breast Cancer BM. (G) L-arginine mediates radiosensitivity through NO-dependent inhibition of GAPDH and PARP activation; (H) Metformin enhances tumor suppression when used as an adjuvant in RT; (I) LRRC31 importation via nanomaterials inhibits DNA repair and radiosensitivity in breast cancer BM; (J) Vorinostat, a histone deacetylase inhibitor, increases radiation sensitivity by inhibiting HDAC; (K) BM secreting S100A9, which binds to the RT-induced RAGE receptor, activates NF-κB-mediated RT resistance.

Table 3. Relevant Parameters of WBRT Research in the AM-BM

Cancer	Species	Injection method	Injection site	Cell line	Cell number/ volume (cells/μl)	Irradiator	Irradiation time (days)	Dose/ Fraction (Gy/F)	Dose rate (Gy/min)	Effect (WBRT vs control)	Ref.
NSCLC	7w Female athymic nude mice	ICB	Left striatum	PC14PE6 H460	1.0×10^4/5	Blood irradiator	14	15/1	2.3	Survival 24/22 days —	[75]
NSCLC	6-8w Female athymic nude mice	ICD	NA	H2030-Br M	5×10^4/100	SARRP (X-Strahl Ltd, Camberley, UK)	After the detection of metastatic lesions by MRI	10/5 10/1	5.2 cGy/s 220kV 13mA	Effects of WBRT on different TAM populations in BrM	[32]
Breast Cancer	5-7w Female athymic nude mice	1. ICD 2. ICB	Right hemisphere	MDA-MB-231-BR	$1.1.75\times10^5$/NA 2.1×10^6/NA	Pentak X-irradiator	1)14-23 2)14	1)30/10 2)15/1	2.53 300 kV 10 mA	30 Gy/10F significantly reduced intracranial metastases, while 15 Gy/1F was more beneficial for median survival	[76]
Breast Cancer	6-8w Female nu/nu mice	ICD	NA	MDA-MB-231-BR	1.5×10^5/100	modified GE eXplore CT 120	26	8/1 16/1 24/1	NA	Mean fractional growth of brain metastases↓ DSB ↑ γ-H2AX ↑ Cell density ↑ nuclear size ↑	[79]
Breast Cancer	6-7w Female BALB/c nu/nu mice	ICD	NA	MDA-MB-231-BR	2×10^5/50	X-RAD 320 orthovoltage irradiator	MRI indicates the brain metastases (about 3W)	12/3	2.33	Tumor volume ↓ Apoptosis ↑	[52]
Breast Cancer	10-12w Female C57BL6/J mice	ICD	NA	99LN-BrM	6×10^4/NA	SARRP	After the detection of metastatic lesions by MRI	10/1	5.2 cGy/s 220 kV 13 mA	WBRT (10 Gy/1F) reduced tumor volume with no significant difference in survival CC3 — Ki67 ↓	[53]
Breast Cancer	6-8w Female nude mice	ICD	NA	MDA-MB-231-BR-HER2	1×10^5/100	integrated micro-computed tomography (CT)/RT system	24 and 25	20/2	0.12 ± 0.01	Mean tumor volume ↓ the number of tumors — total tumor volume — γ-H2AX ↑(DSB)	[54]
Breast Cancer	8 w Female nu/nu mice	ICD	NA	MDA-231-Br	1.75×10^5/100	Xrad-225Cx irradiator (PXi, Cyceron platform)	18	12/3	3.3 225 kV X-rays	αVCAM-1 showed better tumor growth inhibition than WBRT	[87]
1. NSCLC 2. Breast cancer	4–6 w athymic nu/ nu (Harlan) C57BL/6 mice	1. ICD 2. ICB	1. NA 2. Right frontal cortex	1.H2030-Br M 2.E0771-Br M3	1. 1×10^5/100 $2.2.5\times10^4$/2	The irradiator Mark I 30 A	1.7 (30 Gy/10F) 2.3 (30 Gy/10F)	30/10 16.5/3 10/3	NA	*In vivo* OS — *in vitro* S100A9 ↑; RAGE ↑; NF-kB↑; JunB↑; oncosphere CD55+↑	[88]

SRS

SRS, which is commonly administered to single lesions [35,42,72,73] in AM-BM, has received limited research attention. The dosage of SRS tends to decrease when combined with other treatments [35,42]. Numerous studies have demonstrated that SRS contributes to prolonged survival [42,72,73]. Notably, Nakahara et al. recently reported a significant increase in survival when SRS (32 Gy/1F) was combined with immunotherapy [72]. Additionally, they observed the inhibition of JAK2 and STAT3 phosphorylation after SRS (15 Gy/1F). This inhibition, in turn, triggered cell death by regulating apoptosis-related proteins, such as increased Caspase-3 and BAX and decreased BCL-2 and Survivin [42] (**Figure 4C**). A summary of relevant parameters from SRS studies in AM-BM is presented in **Table 4**.

PCI

In contrast to therapeutic irradiation, the primary objective of PCI is to reduce the incidence of BM [25]. This perspective is supported by various preclinical studies and computer models [56,57,78]. In preclinical studies targeting breast cancer, 4 Gy/1F at 3.2 Gy/min and 20 Gy/2F significantly lowered the occurrence of BM [56,78]. However, eliminating dormant cells in BM has shown to be challenging with PCI, which accounts for subsequent tumor occurrence [78].

A critical consideration involves determining the optimal timing for PCI intervention in AM-BM. Studies demonstrate that performing PCI within 1–5 days after tumor cell injection [56,57,78] consistently reduces the incidence of BM. In contrast, executing PCI either before or 3-6 weeks after systemic inoculation poses challenges and may not achieve optimal outcomes [56]. Premature PCI interventions may even promote tumor progression and metastatic formation by inducing alterations in the brain microenvironment. For instance, administering RT (10 Gy/1F) seven days before injection results in damage to normal brain tissue, which becomes more susceptible to the growth of BM [51]. The relevant

parameters of the PCI research are detailed in **Table 5**. Moreover, for those that do not specify the specific radiotherapy method, the parameters are detailed in **Table 6**.

RT and the BBB/BTB

Both clinical and preclinical studies have consistently demonstrated that RT induces an increase in the permeability of the BBB or blood-tumor barrier (BTB), resulting in elevated intracranial drug concentrations. These findings form the theoretical basis for combination therapy [27-29,94-98]. In addition, RT (30 Gy/5F) combined with focused ultrasound (FUS) disrupts BBB integrity [99]. Interestingly, a subset of in-vivo studies has reported contradictory conclusions. Notably, high-dose irradiation whether delivered as a single dose or in a fractionated manner, has shown limited impact on BBB/BTB permeability in certain scenarios [52,54]. In AM-BM of lung/breast cancer (nude mouse models), after 3 Gy/1F [74], 12 Gy/3F [52], 15 Gy/1F [74], 15.5 Gy/1F [100], or 20 Gy/2F [54] irradiation did not significantly alter BBB permeability and, in some cases, even led to a short-term decrease (within 24 hours) [74]. The immune function of the BM model may contribute to this observed phenomenon [100]. For instance, twelve hours after 15.5 Gy/1F irradiation, changes in the integrity of the BBB and the activity of efflux transporters were noted in immunocompetent mice, while no such differences were observed in immunocompromised mice. This finding implies a potential association between the immune response and BBB damage after RT [100]. It is essential to consider the time interval during which RT induces BBB opening, and variations in sensitivity among different detection methods should be taken into account (**Figure 3E**).

Table 4. Relevant Parameters of the SRS Research in the AM-BM

Cancer	Species	Monitoring intracranial tumor formation	Injection method	Injection site	Cell line	Cell number/ volume (cells/ μl)	Irradiator	Irradiation time (days)	Dose/ Fraction (Gy/F)	Dose rate (Gy/ min)	Combination Therapy	Effect	Ref.
NSCLC	7w Female C57BL/ 6 mice	IVIS	ICB	2 mm right lateral and 1 mm posterior of the bregma. The injection depth was adjusted to 3 mm.	LLC	2×10^5/3	Leksell Gamma Knife (LGK)	10	2/1 12.4/2	NA	Nano: HVGGSSV-chitoPEGAcHIS-SP600125 (HVSP-NP)	Tumor size IR ↓ IR+HVSP-NP ↓ ↓ Survival IR ↑ IR+HVSP-NP ↑ ↑ p-JAK (vs IR) IR+HVSP-NP ↓ γH2AX IR+HVSP-NP ↓ Cleaved Caspase3 IR+HVSP-NP ↑	[35]
Melanoma	4-6w Female C57BL/ 6J mice	Volumetric computerized tomography	ICB	Right striatum	B16-F10	5×10^2/ 5	Gamma Knife Model 4C model (Stockholm, Sweden)	4	15/1	2.51	Thymoquinone (TQ) same day as tumor implantation,	*In vivo* Median survival time GK ↑ GK+TQ ↑	[42]
Melanoma	7w male C57BL6 mice	MRI; H&E staining; fluorescent microscopy for GFP	ICB	1 mm anterior and 2 mm lateral to the bregma; lowered to 2.5 mm depth from the surface of the brain	B16-F10	300/1	SARRP	11	18/1	NA	NA	Tumor volumes IR ↓ Survival IR ↑	[73]
Breast Cancer	Fischer 344 rats	NA	ICB	1.8 mm anterior to the bregma and 2 mm to the right of the sagittal suture to a depth of 4 mm below the surface of the skull	MAD B106	5×10^3/5	201-source ^{60}Co Leksell gamma knife	5	32/1	NA	IT:2×10^6 transduced tumor cells vaccination (GM-CSF vaccine or the IL-4 vaccine) 3days	Median survival (vs control) IR ↑ IR+IT ↑ ↑ Infiltration of CD11b/c+ cells SRS ↑ IT ↑ IT + SRS ↑ CD4+cells IT ↑ IT + SRS ↑ αβTCR+ CD8+, and CD28+ cells IT ↑ IT + SRS ↑	[72]

Table 5. Relevant Parameters of the PCI Research in the AM-BM

Cancer	Species	Monitoring intracranial tumor formation	Injection method	Cell line	Cell number/ volume (cells/μl)	Irradiator	Irradiation time (days)	Dose/ Fraction (Gy/F)	Dose rate (Gy/min)	Effect (vs control)	Ref.
Breast Cancer	6-8w Female nude mice	MRI	ICA	MDA-MB-231-BR-HER2	1.75×10^5/100	custom micro-irradiation system	1 and 2	20/2	0.13±0.01	Tumor volume ↓ Tumor number ↓ Non-proliferative cancer cells — (the iron label)	[78]
Breast Cancer	3-5w Female SCID/Beige mice	NA	TVI	MDA-IBC3 (HER2-neu-overexpressing)	5×10^5/NA	NA	2 (before cells were injected) 5, 21, or 42	4/1	NA	The rates of brain metastasis ↓ (5 days)	[57]
Breast Cancer	3-5w Female immunocompromised SCID/ Beige mice (Harlan, USA)	IVIS	TVI	MDA-IBC3	5×10^5/200	X-RAD 225Cx small-animal irradiator (PRECISION X-RAY, North Branford, CT, USA)	2 (before tumor-cell injection) 5 days, 3 weeks, or 6 weeks	4/1	3.2	The rates of brain metastasis ↓ (5 days)	[56]
Breast Cancer	6-8 w Female BALB/c mice	MRI	ICA	4T1-BR5	2×10^4/100	In-house custom micro-irradiation system (140 kVp, 50 kW) with on-board image guidance	7 (before cell delivery)	10/1	NA	Tumor volume and number ↑	[51]
NSCLC	6-8 w male BALB/c nude mice	IVIS	ICD	A549-F3	2×10^5/100	Rad Source Technologies Inc., Suwanee, GA	7 (before cell delivery)	6/2	NA	PCI activates microglia, reduces the localization ability of NSCLC brain metastasis cells	[134]

Table 6. Relevant Parameters of the RT/IMRT in the AM-BM (RT, IMRT, etc.)

Cancer	Species	Injection method	Injection site	Cell line	Cells number/ volume (cells/μl)	Irradiator	Irradiation time (days)	Dose/ fraction (Gy/F)	Dose rate (Gy/ min)	Irradiation method	Combination Therapy	Effect	Ref.
Melanoma	10w nude rats	ICB	Right caudate nucleus	MRA 27	1×10^6/NA	linear accelerator (Siemens Medical Systems, Concord, CA).	12-14	15/3	NA	RT	Boron neutron capture therapy BNCT (BNCT i.v.) BPA (500 mg/kg) containing an equivalent amount of 10B (27 mg B/kg).	Survival: RT ↑; Neutron + RT ↑ ↑; BPA + BNCT+ RT ↑ ↑ ↑; BPA + BNCT +RT ↑ ↑ ↑	[48]
Melanoma	6w Female nude mice	ICB	1 mm anterior to bregma, -1 mm lateral, and -3 mm in deep of the cortex surface	B16-F10	1×10^4/NA	Faxitron CP-160 irradiator	NA	14/7	1.0 Gy/min	IMRT	5-aminolevulinic acid(5-ALA) 200 mg/kg 4 h before X-ray irradiation	*In vivo* Tumor size RT ↓ 5-ALA+RT ↓ ↓ *In vitro* γH2AX RT ↑ 5-ALA+RT ↑ ↑	[101]
Breast Cancer	6w Female BALB/c nude mice	ICB	The brain 2 mm posterior, 1.5 mm right lateral, and 3.5 mm deep from the bregma	MDA-MB-231(Br)	2×10^5/2 PBS	X-Rad 320 (Precision X-Ray, North Branford, CT)	14	15/5	NA	RT	Metformin (300 mg/kg/d) 1 week after Tumor implantation	Metformin increases the concentration of lactate in MDA-MB-231-Br cells by suppressing MCT4 protein, thereby enhancing the antitumor effect of RT	[65]
Breast Cancer	Female Berlin-Druckery IX (BD-IX) rats	ICB	Left striatum	ENU1 564	1×10^3/NA	SARRP irradiator (Xstrahl, Camberley, UK)	20	25 /1	NA 225 kV x-rays	IMRT	NA	Tumor volumes RT ↓	[112]
Breast Cancer	Female immunodeficient nude mice	ICB	Right hemisphere	MDA-MB-231-BR	1×10^5/5 PBS	small-animal radiation research platform (Xstrahl, Camberley, England)	NA	10 /1	2.42 Gy/min 225 kV [peak]	IMRT low-linear energy transfer radiation	Microbubble	Tumor volumes: RT ↓ RT+ O_2 MBs ↓; RT+O_2 MBs + US ↓ ↓ Median Survival: RT ↑; RT+ O_2 MBs ↑; RT+O_2 MBs + US ↑ ↑	[86]
Breast Cancer	4-6w Female	ICB	Caudate nucleus	MDA-MB-2	1×10^6/5	Pantak irradiator	3	5 /1	2.28 Gy/min	RT	TT: vorinostat (75 mg/kg)	*In vivo* Tumor volume	[47]

Cancer	Species	Injection method	Injection site	Cell line	Cells number/ volume (cells/μl)	Irradiator	Irradiation time (days)	Dose/ fraction (Gy/F)	Dose rate (Gy/ min)	Irradiation method	Combination Therapy	Effect	Ref.
	nude mice			31-BR								RT ↓ RT +vorinostat ↓ ↓ Survival RT ↑ RT +vorinostat ↑ ↑ *In vitro* γH2AX RT ↑ RT +vorinostat ↑ ↑ Mitotic catastrophe RT ↑ RT +vorinostat ↑ ↑	

Table 7. A Comprehensive and Scientific Template for Reporting Experiments Involving Animal Models of Brain Metastasis Radiotherapy

Parameter	Notes on Reporting
Study design	
Assessment time-points post-irradiation	in Weeks
Serial assessment of >=1 parameter completed?	Yes/No
Combination therapy	Immunotherapy, Chemotherapy, Targeted therapy
Sequence of combination therapy	–
Tumor parameters	
Tumor type	Lung cancer, Breast cancer, Melanoma
Injection method	Orthotopic injection, Intracardiac injection, Carotid artery injection, Tail vein injection
Time of cell injection	in Weeks
Number of tumor cells	–
Cell line	A549, LLC, 4T1, B16-F10
Injection site	Frontal lobe, Striatum
Tumor size	
Radionuclide imaging	Yes/No
Magnetic resonance imaging (MRI)	Yes/No
Bioluminescence imaging (BLI)	Yes/No
CT/PET-CT	Yes/No
Animal character	
Animal species	Mouse or Rat
Animal strain	C57BL/6, BLAB/c, SCID, SD
Sex	Male or Female
Gene modifications/ spontaneous mutations	–
Irradiation	
Irradiation time (after/before irradiation)	in Weeks
Target volume	Whole Body, Head, Whole Brain, or Partial Brain
Form of ionizing radiation	X-rays, Gamma rays, Electrons, Heavy ions
Energy of radiation	in kV or MV
Dose rate	in Gy/min
Field arrangement	–
Radiation device used	Brand & Model
Dose fractionation	
Total physical irradiation dose	in Gray
Total fractions	–
Duration over which irradiation was given	in Days
Functional analyses	
Blood-brain barrier permeability	Yes/No
Animal weight	Yes/No
Tumor size	Yes/No
Radiotherapy-related markers	Yes/No
Invasive hemodynamics	Yes/No
Tumor markers	Yes/No
Radiography	Yes/No

Combination therapy in AM-BM

RT Combined with Chemotherapy

Chemotherapy has been shown to augment the radiosensitivity of BM [50,55,101,102]. Temozolomide (TMZ) [55,102], etoposide [50], and dexrazoxane [50], when combined with RT, effectively inhibit the progression of AM-BM. TMZ, recognized for its ability to penetrate the blood-brain barrier, is recommended as a chemotherapeutic drug for intracranial tumors [103]. Furthermore, TMZ enhances the radiosensitivity of brain metastatic tumor cells by inhibiting DNA damage repair after RT and amplifying mitotic catastrophe [102]. RT combined with TMZ has been shown to prolong survival in AM-BM of breast cancer [55]. Meanwhile, in the AM-BMs of NSCLC, non-ablative radiation (2 Gy) enhances the delivery of anti-MGMT morpholino oligonucleotides (AMONs) improving TMZ efficacy by inhibiting MGMT [43]. Etoposide plus dexrazoxane, combined with WBRT (10 Gy/1F) increased the median survival by 60% with no additional toxicity [50]. Similarly, an antibody-drug conjugate such as BR96-DOX in combination with RT significantly prolonged survival in AM-BMs of SCLC [77]. Furthermore, compared with concurrent chemoradiotherapy, antibody-drug conjugates administered before RT improved survival [77].

RT Combined with Targeted Therapy

The combination of RT and targeted therapy typically has synergistic effects [104]. WBRT enhances the therapeutic effect of single domain antibody fragment (Anti-HER2 VHH 5F7) on human epidermal growth factor receptor type 2 (HER2) positive BM by increasing vascular permeability [49]. Overall, targeted c-Met and RT inhibit tumors and prolong the overall survival of tumor-bearing mice [44].

Similarly, targeted agents enhance the efficacy of radiotherapy. Targeting EGFR [62], CHK1 [45], HDAC [47], CXCR4 [71], ATR [47], and GRM1 [82] significantly improved RT efficacy. For instance, AZD3759 (zorifertinib) amplifies the antitumor effect of RT by interfering with EGFR and JAK1 [62] (**Figure 4A**).

AZD7762 enhances radiosensitivity *in vitro* and *in vivo* by inhibiting CHK1 [45] (**Figure 4B**). Vorinostat improves the median survival of AM-BMs by blocking histone deacetylases (HDACs), leading to DSBs repair inhibition and mitotic catastrophe [47] (**Figure 4J**). Riluzole (a glutamate signaling blockade) sensitized cells to RT (**Figure 4E**). Mechanistically, inhibition of glutamate signaling led to G2/M phase arrest in melanoma cells [82].

Additionally, targeted drugs modulate the tumor microenvironment [71,82]. Endostar enhances RT efficacy by blocking RT-induced CXCR4. Subsequently, TAM infiltration and macrophage M2 polarization are inhibited, and the percentage of CD4+T/CD3+T cells increases [71].

RT Combined with Immunotherapy

Immunotherapeutic strategies, including immune checkpoint inhibition (ICI), adoptive cells, tumor vaccines, oncolytic viruses, and cytokine therapy, are integral components of AM-BM treatment. Currently, the integration of immunotherapy with RT in AM-BM primarily involves ICI and *in-situ* vaccination (ISV), both of which enhance RT efficacy. Notably, combining a tumor vaccine with RT (15 Gy) significantly reduces tumor volume and delays BM progression [33].

RT contributes to immunotherapy efficacy by regulating the tumor microenvironment [30-32]. WBRT recruits myeloid cells and enhances their proinflammatory response [32]. Meanwhile, WBRT significantly elevated TNF-α and CXCL1 in the serum of immunocompetent and immunocompromised mice [100]. The levels of proinflammatory cytokines (TNF-α, IL-2, and IL-12p70) increase after WBRT in immunocompetent mice but not in nude mice [100]. Furthermore, increasing the radiation dose (from 15 Gy to 18.5 Gy) improved immunotherapy efficacy in AM-BM, resulting in longer survival and tumor dormancy periods [34]. Relatively low-dose WBRT (4 Gy) or targeted radionuclide therapy increased the number of T cells (CD4+ and CD8+) and the monocyte/macrocytic phagocytic (F4/80+) population, enhancing the immunotherapy response in melanoma BM [30].

The sequencing of immunotherapy and RT needs to be further explored. Transcriptome analysis revealed that RT following ICI treatment is involved in cell death and inflammation signaling in melanoma BM. Preclinical studies have demonstrated that RT followed by anti-PD-L1 therapy is preferable [105], which has also been confirmed in clinical trials [106, 107].

Combination of RT and Novel Technologies

Ongoing exploration by radiation biologists has led to the application of novel technologies to AM-BM. Compared with conventional RT, FLASH radiotherapy (FLASH-RT) and heavy ion radiotherapy exhibit superior curative effects with relatively fewer adverse events [108], holding promise for BM treatment [109].

The optimization of drug carriers has also advanced the field of BMs treatment. RT combined with ultrasound-mediated rupture of oxygen-carrying microbubbles (MBs) delays tumor progression and improves survival in AM-BM of breast cancer [86]. In addition, nanoparticles enhance the therapeutic effect of RT on BM by modulating radiosensitivity [35-37] or increasing the dose absorption of RT [38] (**Figure 4I**).

The development of novel medicines is equally compelling for researchers. 5-aminolevulinic acid (5-ALA), a novel photodynamic drug, enhances the radiosensitivity of melanoma BM by upregulating protoporphyrin IX (PpIX) [101] (**Figure 4F**). Thymoquinone (TQ) improves the efficacy of gamma knife therapy on melanoma BMs, by enhancing apoptosis through regulation of the JAK2/STAT3 pathway [42]. Moreover, TQ induces the secretion of inflammatory growth factors [42] (**Figure 4D**). Metformin increases the concentration of lactate in MDA-MB-231-Br cells by suppressing the MCT4 protein, thereby enhancing the anti-tumor effect of RT [65] (**Figure 4H**). In the AM-BM of breast cancer, L-arginine amplifies RT efficacy by modulating nitric oxide metabolism [110] (**Figure 4G**). Additionally, magnetic field therapy (athermal radiofrequency electromagnetic fields) combined with RT significantly inhabits radiation-resistant cells and prolongs the survival of AM-BMs [111].

Future and Prospects

The two-year survival rate for patients with BM is typically less than 10% [12]. RT, including WBRT and SRS, is one of the essential treatments for BM. The topic of brain metastases has attracted much attention in the 2023 oncology conferences (such as ASCO, ASTRO, and WCLC). Dose exploration remains a key topic, particularly in the field of radiotherapy for brain metastases. This review, based on the AM-BM of various tumors, presents a comprehensive summary of preclinical research on BM and RT for the first time. We focused on RT parameters, including modality, total dose, fractionation, dose rate, and their corresponding effects. Additionally, we highlight recent advancements in the study of BM with RT, emphasizing combination with chemotherapy, targeted therapy, immunotherapy, and novel technologies.

Animal models for BM encompass diverse species, including mice [30,38,41,43,49,56,60-65], rats [48,72,77,112, 113], monkeys [114], dogs [115], rabbits [116], and chick

embryos [117-119], with mice being predominantly the predominant ones used (**Figure 3A**). The organ tropism of tumor cells in chick embryos was recently found to be consistent with that in mice [118]. The location of the BM in most studies is limited to the cerebral cortex [49, 50] or the striatum [33, 39, 41-48]. Establishing the AM-BMs in specific anatomical locations, such as the leptomeninges [120, 121] and cerebellum [122], requires further exploration. The "seed" and "soil" interactions during tumor metastasis endow the primary tumors and metastases with different characteristics, the selection and establishment of brain-tropic cells necessitate attention [68]. Radiation-resistant models have also received limited research attention. In recent years, the application of humanized mice, microfluidic chips mimicking [123, 124], PDX models [39,40], and organoids [125] has emerged, enhancing the translatability of research in the field of BM. The application of emerging models, diagnostic methods, and treatment techniques to study brain metastasis may catalyze its clinical transformation and change treatment paradigms, which deserves further attention. Single-cell sequence and spatial transcriptomics offer promising avenues for obtaining more authentic information about BMs. Meanwhile, the difference in the organ affinity of primary tumor metastases to brain tissue needs to be further explored. Owing to the rarity of brain metastatic cells, certain studies have resorted to employing cell lines derived from primary tumors to investigate the relevant mechanisms involved. Although validated in animal models, the exploration of brain metastasis mechanisms outside the brain microenvironment has somewhat compromised the persuasiveness of the conclusions. This issue is currently a focus in the field of brain metastasis research. Continuous optimization of animal model construction and the development of emerging models may offer a potential solution.

For clinical transformation, preclinical studies have mostly used mice, which have certain differences in genetics, radiation sensitivity, and other aspects compared to humans. Like the parameters of chemotherapy and immunotherapy, preclinical radiation dosimetry parameters are difficult to convert and apply to humans. In terms of dosage, preclinical models can only provide positive (effective tumor suppression) or negative (failure to tumor suppression) results, which is an unavoidable problem in clinical transformation. Utilizing and optimizing models with personalized patient information, such as PDX models and organoids, is more convincing and easier to use for achieving clinical conversion.

The choice of the RT method is influenced by the establishment of animal models. BM formed by intracerebral inoculation is commonly treated with WBRT or SRS, whereas intracardiac and carotid artery injections (systemic injection) may generate multiple intracranial metastases, often treated with WBRT in AM-BM. In addition, intravenous injection is relatively more frequently used in PCI research. However, whether the carotid artery or intracardiac injection is suitable for PCI research still needs convincing evidence.

The timing of RT intervention is also worthy of attention. The AM-BMs of breast/lung cancer (10^6 tumor cells) or melanoma (10^4 tumor cells) constructed by intracerebral injection are generally administrated RT within two weeks. Meanwhile, for systemic inoculation, the irradiation time for intracardiac injection modeling is generally later than that for intracerebral transplantation. Notably, the timing of RT intervention and the definition of the irradiation field between AM-BM and clinical application pose challenges but advances in animal imaging technology and RT may provide solutions.

Current RT regimens for AM-BM include four criteria: (1) clinical regimens [62,74,76], (2) BED equivalent regimens [33,34,38,45,54,75,76,79], (3) experience-based regimens [35-37,52,56], and (4) protection of normal tissues [49,55,82]. Dose and fractionation emerge as critical factors. Presently, BED equivalent schemes (based on the L-Q model) are predominantly applied. Most studies employ either single high-dose irradiation or high-dose fractional irradiation (15-16 Gy/1F) [33,34,38,45,54,75,76,79]. However, some researchers argue that the L-Q model is unsuitable for high-dose irradiation [126], in which the dose-survival curve of tumor cells is significantly shifted, accounting for decreased predictive accuracy [81,92]. Meanwhile, for BED calculations, α/β is not entirely consistent across different tumors and cell subtypes [91]. While RT alone or combined with other treatments effectively inhibits BM, inevitable adverse events, including radiation necrosis, cerebral edema, and neuronal damage, can occur [127]. Due to the substantial heterogeneity among various studies, drawing definitive conclusions regarding optimal RT regimens or combination therapies for maximum benefit is challenging.

Owing to the limited volume of BM in animals, only a few preclinical studies have reported IMRT in AM-BM [86,128]. Conformal magnetic resonance imaging (MRI) in rats contributes to precise RT to some extent [112]. Currently, the Small Animal Radiation Research Platform (SARRP) (Xstrahl, Camberley, UK) [129,130], X-RAD SmART (Precision X-ray, North Branford, Connecticut, USA) [131], and the SAIGRT system [132] have been validated to achieve small-volume precise radiotherapy in AM-BM. Moreover, Delaney et al. conducted IMRT for mice BMs using

SARRP combined with cone-beam computed tomography guidance [86]. Interestingly, they demonstrated that the clinical linear accelerator Novalis TX (Brainlab AG, Feldkirchen, Germany) could also achieve IMRT in AM-BM [128].

Innovative irradiation methods such as HA-WBRT, FLASH-RT [108], and heavy iron therapy [109], may yield improved therapeutic effects in BM. Recent studies have explored tumor-treating fields [133] and athermal radiofrequency electromagnetic field [111]. Targeted therapy, immunotherapy, and novel technologies like nanoparticles and oxygen-containing microbubbles have been extensively studied in primary tumors, but their exploration in metastatic tumors is limited (**Figure 5**). Tumor cells evolve during metastatic periods, and the characteristics of metastatic lesions are not consistent with those of primary tumors. Moreover, the BBB establishes a particular intracranial immune environment. Consequently, the application of novel treatment methods and technologies for treating BM warrants further investigation. The mechanisms by which RT modulates the BBB and regulates the microenvironment of the BM demand in-depth exploration.

In conclusion, the choice of RT regimens in BM depends on the model establishment. It is imperative to focus on refining RT or comprehensive treatment protocols for AM-BM and strive for the standardization of preclinical research on RT to facilitate its clinical application. However, further studies are needed to elucidate how to optimize the efficacy of RT in BM.

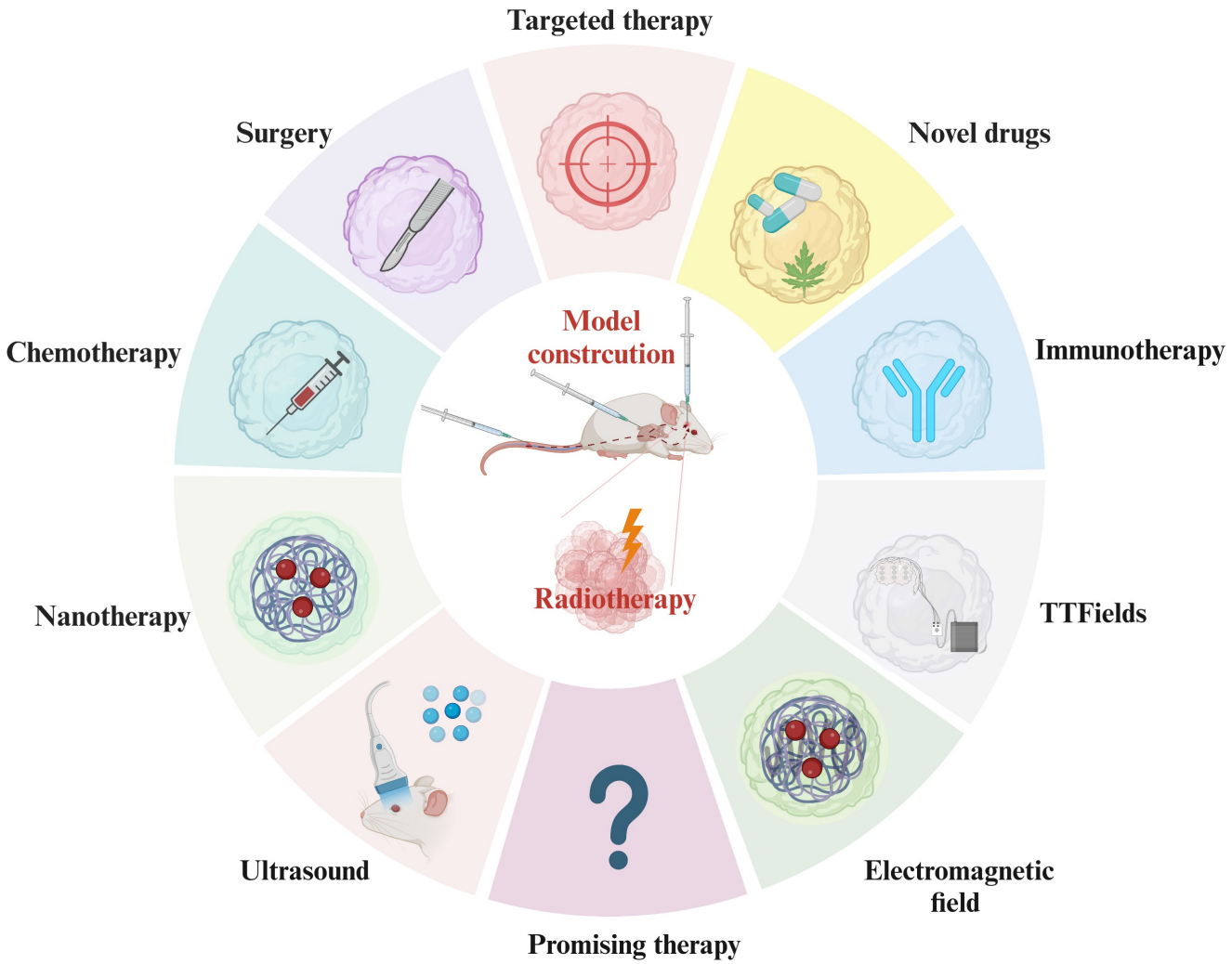

Figure 5. Combination Treatment with RT in Current AM-BM Research. Current research on AM-BMs explores diverse combination treatments with RT, including immunotherapy, novel drug applications, targeted therapy, surgery, chemotherapy, nanomaterial applications, ultrasound (mediating oxygen-containing microbubble rupture), magnetic field therapy, and electric field therapy. These comprehensive approaches signify the multifaceted strategies being investigated to optimize the efficacy of RT in AM-BM.

Abbreviations

BMs: brain metastases; AM-BM: animal model of brain metastases; WBRT: whole brain radiation therapy; SRS: stereotactic radiosurgery; PCI: prophylactic cranial irradiation; RT: Radiotherapy; IMRT: Intensity-modulated radiation therapy; ICB: intracerebral injection; ICD: intracardiac injection; ICA: intracarotid artery injection; IV: Intravenous inoculations; TVI: tail vein injection; PDX: Patient-derived tumor xenograft; MRI: magnetic resonance imaging; BBB: the blood-brain barrier; L-Q: The linear-quadratic; BED: the Biologically effective dose; D: total Dose; d: single dose; TAM-MDM: monocyte-derived macrophages; TAM-MDM: monocyte-derived macrophages; BTB: blood-tumor barrier; FUS: focused ultrasound; TMZ: temozolomide; NSCLC: non-small cell lung cancer; AMONs: anti-MGMT morpholino oligonucleotides; EGFR: Epidermal growth factor receptor; HER2: growth factor receptor type 2; HDACs: Histone deacetylases; ES: Endostar; ICI: immune checkpoint inhibitors; ISV: *in situ* vaccination; IVIS: *In vivo* Imaging System; NF-κB: nuclear factor kappa-light-chain-enhancer of Activated B cells signaling; FLASH-RT: FLASH radiotherapy; RAGE: receptor for advanced glycation end products; MBs: microbubbles; 5-ALA: 5-aminolevulinic acid; PpIX: protoporphyrin IX; TQ: Thymoquinone; GRM1: metabotropic glutamate receptor 1; SARRP: the Small Animal Radiation Research Platform.; LLC: Lewis lung cancer; IT: immunotherapy; TT: targeted therapy; CTR: Chemotherapy; GK: Gamma Knife; NA: Not available.

Acknowledgments

We thank the team members for their valuable and constructive comments. Also, we thank all those involved in writing and revising this manuscript. Also, we thank members of Hunan SJA laboratory animal Co., Ltd. for their help. The figures are created with BioRender.com.

Funding

This work was supported by the Natural Science Foundation of Hunan (2022JJ30992 to R.R.Z) and the National Multidisciplinary Cooperative Diagnosis and Treatment Capacity Building Project for Major Diseases of China (Lung Cancer, z027002).

Availability of data and materials

Data sharing does not apply to this article as no datasets were generated or analyzed during the current study.

Author contributions

WS collected the original data, performed the literature review, wrote the manuscript, and revised the tables. GT conceived the structure of the manuscript and critically revised the manuscript. LC and WHJ designed figures. JN, XG, and HP revised the tables. DJ, HL, JN, and MY made critical revisions, modified the grammar, and polished the paper. WS and GT contributed equally to the manuscript. All authors reviewed and approved the final manuscript to be published.

Competing Interests

The authors have declared that no competing interest exists.

References

1. Arvold ND, Lee EQ, Mehta MP, Margolin K, Alexander BM, Lin NU, et al. Updates in the management of brain metastases. Neuro Oncol. 2016; 18: 1043-65.
2. Liu W, Powell CA, Wang Q. Tumor microenvironment in lung cancer-derived brain metastasis. Chin Med J (Engl). 2022; 135: 1781-91.
3. Jin Y, Kang Y, Wang M, Wu B, Su B, Yin H, et al. Targeting polarized phenotype of microglia via IL6/JAK2/STAT3 signaling to reduce NSCLC brain metastasis. Signal Transduct Target Ther. 2022; 7: 52.
4. Martin AM, Cagney DN, Catalano PJ, Warren LE, Bellon JR, Punglia RS, et al. Brain Metastases in Newly Diagnosed Breast Cancer: A Population-Based Study. JAMA Oncol. 2017; 3: 1069-77.
5. Zhang Q, Abdo R, Iosef C, Kaneko T, Cecchini M, Han VK, et al. The spatial transcriptomic landscape of non-small cell lung cancer brain metastasis. Nat Commun. 2022; 13: 5983.
6. Sperduto PW, Yang TJ, Beal K, Pan H, Brown PD, Bangdiwala A, et al. Estimating Survival in Patients With Lung Cancer and Brain Metastases: An Update of the Graded Prognostic Assessment for Lung Cancer Using Molecular Markers (Lung-molGPA). JAMA Oncol. 2017; 3: 827-31.
7. Wood SL, Pernemalm M, Crosbie PA, Whetton AD. The role of the tumor-microenvironment in lung cancer-metastasis and its relationship to potential therapeutic targets. Cancer Treat Rev. 2014; 40: 558-66.
8. Corti C, Antonarelli G, Criscitiello C, Lin NU, Carey LA, Cortés J, et al. Targeting brain metastases in breast cancer. Cancer Treat Rev. 2022; 103: 102324.
9. Xing F, Liu Y, Wu SY, Wu K, Sharma S, Mo YY, et al. Loss of XIST in Breast Cancer Activates MSN-c-Met and Reprograms Microglia via Exosomal miRNA to Promote Brain Metastasis. Cancer Res. 2018; 78: 4316-30.
10. Kleffman K, Levinson G, Rose IVL, Blumenberg LM, Shadaloey SAA, Dhabaria A, et al. Melanoma-Secreted Amyloid Beta Suppresses Neuroinflammation and Promotes Brain Metastasis. Cancer Discov. 2022; 12: 1314-35.
11. Siegel RL, Miller KD, Jemal A. Cancer statistics, 2019. CA Cancer J Clin. 2019; 69: 7-34.
12. Matsui JK, Perlow HK, Baiyee C, Ritter AR, Mishra MV, Bovi JA, et al. Quality of Life and Cognitive Function Evaluations and Interventions for Patients with Brain Metastases in the Radiation Oncology Clinic. Cancers (Basel). 2022; 14.
13. Boire A, Brastianos PK, Garzia L, Valiente M. Brain metastasis. Nat Rev Cancer. 2020; 20: 4-11.
14. Narloch JL, Farber SH, Sammons S, McSherry F, Herndon JE, Hoang JK, et al. Biopsy of enlarging lesions after stereotactic radiosurgery for brain metastases frequently reveals radiation necrosis. Neuro Oncol. 2017; 19: 1391-7.
15. McTyre E, Scott J, Chinnaiyan P. Whole brain radiotherapy for brain metastasis. Surg Neurol Int. 2013; 4: S236-44.
16. Mahajan A, Ahmed S, McAleer MF, Weinberg JS, Li J, Brown P, et al. Post-operative stereotactic radiosurgery versus observation for completely resected brain metastases: a single-centre, randomised, controlled, phase 3 trial. Lancet Oncol. 2017; 18: 1040-8.
17. Brown PD, Ballman KV, Cerhan JH, Anderson SK, Carrero XW, Whitton AC, et al. Postoperative stereotactic radiosurgery compared with whole brain radiotherapy for resected metastatic brain disease (NCCTG N107C/CEC 3): a multicentre, randomised, controlled, phase 3 trial. Lancet Oncol. 2017; 18: 1049-60.
18. Yamamoto M, Serizawa T, Shuto T, Akabane A, Higuchi Y, Kawagishi J, et al. Stereotactic radiosurgery for patients with multiple brain metastases (JLGK0901): a multi-institutional prospective observational study. Lancet Oncol. 2014; 15: 387-95.
19. Sperduto PW, Shanley R, Luo X, Andrews D, Werner-Wasik M, Valicenti R, et al. Secondary analysis of RTOG 9508, a phase 3 randomized trial of

whole-brain radiation therapy versus WBRT plus stereotactic radiosurgery in patients with 1-3 brain metastases; poststratified by the graded prognostic assessment (GPA). Int J Radiat Oncol Biol Phys. 2014; 90: 526-31.
20. Tsao MN, Rades D, Wirth A, Lo SS, Danielson BL, Gaspar LE, et al. Radiotherapeutic and surgical management for newly diagnosed brain metastasis(es): An American Society for Radiation Oncology evidence-based guideline. Pract Radiat Oncol. 2012; 2: 210-25.
21. Kayama T, Sato S, Sakurada K, Mizusawa J, Nishikawa R, Narita Y, et al. Effects of Surgery With Salvage Stereotactic Radiosurgery Versus Surgery With Whole-Brain Radiation Therapy in Patients With One to Four Brain Metastases (JCOG0504): A Phase III, Noninferiority, Randomized Controlled Trial. J Clin Oncol. 2018: Jco2018786186.
22. Vogelbaum MA, Brown PD, Messersmith H, Brastianos PK, Burri S, Cahill D, et al. Treatment for Brain Metastases: ASCO-SNO-ASTRO Guideline. J Clin Oncol. 2022; 40: 492-516.
23. Zhang W, Jiang W, Luan L, Wang L, Zheng X, Wang G. Prophylactic cranial irradiation for patients with small-cell lung cancer: a systematic review of the literature with meta-analysis. BMC Cancer. 2014; 14: 793.
24. Crockett C, Belderbos J, Levy A, McDonald F, Le Péchoux C, Faivre-Finn C. Prophylactic cranial irradiation (PCI), hippocampal avoidance (HA) whole brain radiotherapy (WBRT) and stereotactic radiosurgery (SRS) in small cell lung cancer (SCLC): Where do we stand? Lung Cancer. 2021; 162: 96-105.
25. Péchoux CL, Sun A, Slotman BJ, De Ruysscher D, Belderbos J, Gore EM. Prophylactic cranial irradiation for patients with lung cancer. Lancet Oncol. 2016; 17: e277-e93.
26. Scoccianti S, Ricardi U. Treatment of brain metastases: review of phase III randomized controlled trials. Radiother Oncol. 2012; 102: 168-79.
27. Sprowls SA, Arsiwala TA, Bumgarner JR, Shah N, Lateef SS, Kielkowski BN, et al. Improving CNS Delivery to Brain Metastases by Blood-Tumor Barrier Disruption. Trends Cancer. 2019; 5: 495-505.
28. Khalifa J, Amini A, Popat S, Gaspar LE, Faivre-Finn C. Brain Metastases from NSCLC: Radiation Therapy in the Era of Targeted Therapies. J Thorac Oncol. 2016; 11: 1627-43.
29. Oberoi RK, Parrish KE, Sio TT, Mittapalli RK, Elmquist WF, Sarkaria JN. Strategies to improve delivery of anticancer drugs across the blood-brain barrier to treat glioblastoma. Neuro-Oncology. 2016; 18: 27-36.
30. Clark PA, Sriramaneni RN, Bates AM, Jin WJ, Jagodinsky JC, Hernandez R, et al. Low-Dose Radiation Potentiates the Propagation of Anti-Tumor Immunity against Melanoma Tumor in the Brain after *In situ* Vaccination at a Tumor outside the Brain. Radiat Res. 2021; 195: 522-40.
31. Niesel K, Schulz M, Anthes J, Alekseeva T, Macas J, Salamero-Boix A, et al. The immune suppressive microenvironment affects efficacy of radio-immunotherapy in brain metastasis. EMBO Mol Med. 2021; 13: e13412.
32. Schulz M, Michels B, Niesel K, Stein S, Farin H, Rödel F, et al. Cellular and Molecular Changes of Brain Metastases-Associated Myeloid Cells during Disease Progression and Therapeutic Response. iScience. 2020; 23: 101178.
33. Smilowitz HM, Sasso D, Lee EW, Goh G, Micca PL, Dilmanian FA. Therapy model for advanced intracerebral B16 mouse melanoma using radiation therapy combined with immunotherapy. Cancer Immunol Immunother. 2013; 62: 1187-97.
34. Smilowitz HM, Micca PL, Sasso D, Wu Q, Dyment N, Xue C, et al. Increasing radiation dose improves immunotherapy outcome and prolongation of tumor dormancy in a subgroup of mice treated for advanced intracerebral melanoma. Cancer Immunol Immunother. 2016; 65: 127-39.
35. Lim SH, Li CH, Jeong YI, Jang WY, Choi JM, Jung S. Enhancing Radiotherapeutic Effect With Nanoparticle-Mediated Radiosensitizer Delivery Guided By Focused Gamma Rays In Lewis Lung Carcinoma-Bearing Mouse Brain Tumor Models. Int J Nanomedicine. 2019; 14: 8861-74.
36. Kotb S, Detappe A, Lux F, Appaix F, Barbier EL, Tran VL, et al. Gadolinium-Based Nanoparticles and Radiation Therapy for Multiple Brain Melanoma Metastases: Proof of Concept before Phase I Trial. Theranostics. 2016; 6: 418-27.
37. Chen Y, Jiang T, Zhang H, Gou X, Han C, Wang J, et al. LRRC31 inhibits DNA repair and sensitizes breast cancer brain metastasis to radiation therapy. Nat Cell Biol. 2020; 22: 1276-85.
38. Hainfeld JF, Ridwan SM, Stanishevskiy FY, Smilowitz HM. Iodine nanoparticle radiotherapy of human breast cancer growing in the brains of athymic mice. Sci Rep. 2020; 10: 15627.
39. Baschnagel AM, Kaushik S, Durmaz A, Goldstein S, Ong IM, Abel L, et al. Development and characterization of patient-derived xenografts from non-small cell lung cancer brain metastases. Sci Rep. 2021; 11: 2520.
40. Camphausen K, Purow B, Sproull M, Scott T, Ozawa T, Deen DF, et al. Influence of *in vivo* growth on human glioma cell line gene expression: convergent profiles under orthotopic conditions. Proc Natl Acad Sci U S A. 2005; 102: 8287-92.
41. Chu C, Davis CM, Lan X, Hienz RD, Jablonska A, Thomas AM, et al. Neuroinflammation After Stereotactic Radiosurgery-Induced Brain Tumor Disintegration Is Linked to Persistent Cognitive Decline in a Mouse Model of Metastatic Disease. Int J Radiat Oncol Biol Phys. 2020; 108: 745-57.
42. Hatiboglu MA, Kocyigit A, Guler EM, Akdur K, Khan I, Nalli A, et al. Thymoquinone Enhances the Effect of Gamma Knife in B16-F10 Melanoma Through Inhibition of Phosphorylated STAT3. World Neurosurg. 2019; 128: e570-e81.
43. Ambady P, Wu YJ, Kersch CN, Walker JM, Holland S, Muldoon LL, et al. Radiation enhances the delivery of antisense oligonucleotides and improves chemo-radiation efficacy in brain tumor xenografts. Cancer Gene Ther. 2022; 29: 533-42.
44. Yang H, Lee HW, Kim Y, Lee Y, Choi YS, Kim KH, et al. Radiosensitization of brain metastasis by targeting c-MET. Lab Invest. 2013; 93: 344-53.
45. Yang H, Yoon SJ, Jin J, Choi SH, Seol HJ, Lee JI, et al. Inhibition of checkpoint kinase 1 sensitizes lung cancer brain metastases to radiotherapy. Biochem Biophys Res Commun. 2011; 406: 53-8.
46. Baschnagel AM, Elnaggar JH, VanBeek HJ, Kromke AC, Skiba JH, Kaushik S, et al. ATR Inhibitor M6620 (VX-970) Enhances the Effect of Radiation in Non-Small Cell Lung Cancer Brain Metastasis Patient-Derived Xenografts. Mol Cancer Ther. 2021; 20: 2129-39.
47. Baschnagel A, Russo A, Burgan WE, Carter D, Beam K, Palmieri D, et al. Vorinostat enhances the radiosensitivity of a breast cancer brain metastatic cell line grown *in vitro* and as intracranial xenografts. Mol Cancer Ther. 2009; 8: 1589-95.
48. Barth RF, Grecula JC, Yang W, Rotaru JH, Nawrocky M, Gupta N, et al. Combination of boron neutron capture therapy and external beam radiotherapy for brain tumors. Int J Radiat Oncol Biol Phys. 2004; 58: 267-77.
49. Procissi D, Jannetti SA, Zannikou M, Zhou Z, McDougald D, Kanojia D, et al. Low-level whole-brain radiation enhances theranostic potential of single-domain antibody fragments for human epidermal growth factor receptor type 2 (HER2)-positive brain metastases. Neurooncol Adv. 2022; 4: vdac135.
50. Hofland KF, Thougaard AV, Dejligbjerg M, Jensen LH, Kristjansen PE, Rengtved P, et al. Combining etoposide and dexrazoxane synergizes with radiotherapy and improves survival in mice with central nervous system tumors. Clin Cancer Res. 2005; 11: 6722-9.
51. Hamilton AM, Wong SM, Wong E, Foster PJ. Cranial irradiation increases tumor growth in experimental breast cancer brain metastasis. NMR Biomed. 2018; 31: e3907.
52. Crowe W, Wang L, Zhang Z, Varagic J, Bourland JD, Chan MD, et al. MRI evaluation of the effects of whole brain radiotherapy on breast cancer brain metastasis. Int J Radiat Biol. 2019; 95: 338-46.
53. Chae WH, Niesel K, Schulz M, Klemm F, Joyce JA, Prümmer M, et al. Evaluating Magnetic Resonance Spectroscopy as a Tool for Monitoring Therapeutic Response of Whole Brain Radiotherapy in a Mouse Model for Breast-to-Brain Metastasis. Front Oncol. 2019; 9: 1324.
54. Murrell DH, Zarghami N, Jensen MD, Chambers AF, Wong E, Foster PJ. Evaluating Changes to Blood-Brain Barrier Integrity in Brain Metastasis over Time and after Radiation Treatment. Transl Oncol. 2016; 9: 219-27.
55. Martínez-Aranda A, Hernández V, Picón C, Modolell I, Sierra A. Development of a preclinical therapeutic model of human brain metastasis with chemoradiotherapy. Int J Mol Sci. 2013; 14: 8306-27.
56. Smith DL, Debeb BG, Diagaradjane P, Larson R, Kumar S, Ning J, et al. Prophylactic cranial irradiation reduces the incidence of brain metastasis in a mouse model of metastatic, HER2-positive breast cancer. Genes Cancer. 2021; 12: 28-38.
57. Smith DL, Debeb BG, Thames HD, Woodward WA. Computational Modeling of Micrometastatic Breast Cancer Radiation Dose Response. Int J Radiat Oncol Biol Phys. 2016; 96: 179-87.
58. Kim SH, Redvers RP, Chi LH, Ling XW, Lucke AJ, Reid RC, et al. Identification of brain metastasis genes and therapeutic evaluation of histone deacetylase inhibitors in a clinically relevant model of breast cancer brain metastasis. Disease Models & Mechanisms. 2018; 11.
59. Daphu I, Sundstrøm T, Horn S, Huszthy PC, Niclou SP, Sakariassen P, et al. *In vivo* animal models for studying brain metastasis: value and limitations. Clin Exp Metastasis. 2013; 30: 695-710.
60. Black PJ, Smith DR, Chaudhary K, Xanthopoulos EP, Chin C, Spina CS, et al. Velocity-based Adaptive Registration and Fusion for Fractionated Stereotactic Radiosurgery Using the Small Animal Radiation Research Platform. Int J Radiat Oncol Biol Phys. 2018; 102: 841-7.
61. Cho JH, Robinson JP, Arave RA, Burnett WJ, Kircher DA, Chen G, et al. AKT1 Activation Promotes Development of Melanoma Metastases. Cell Rep. 2015; 13: 898-905.
62. Zhao R, Yin W, Yu Q, Mao Y, Deng Q, Zhang K, et al. AZD3759 enhances radiation effects in non-small-cell lung cancer by a synergistic blockade of epidermal growth factor receptor and Janus kinase-1. Bioengineered. 2022; 13: 331-44.
63. De Meulenaere V, Descamps B, De Wever O, Vanhove C, Deblaere K. *In vivo* selection of the MDA-MB-231br/eGFP cancer cell line to obtain a clinically relevant rat model for triple negative breast cancer brain metastasis. PLoS One. 2020; 15: e0243156.
64. Ridwan SM, Hainfeld JF, Ross V, Stanishevskiy Y, Smilowitz HM. Novel Iodine nanoparticles target vascular mimicry in intracerebral triple negative human MDA-MB-231 breast tumors. Sci Rep. 2021; 11: 1203.
65. Choi YS, Lee J, Lee HS, Song JE, Kim DH, Song HT. Offset of apparent hyperpolarized (13) C lactate flux by the use of adjuvant metformin in ionizing radiation therapy *in vivo*. NMR Biomed. 2021; 34: e4561.
66. Serres S, Martin CJ, Sarmiento Soto M, Bristow C, O'Brien ER, Connell JJ, et al. Structural and functional effects of metastases in rat brain determined by multimodal MRI. Int J Cancer. 2014; 134: 885-96.
67. Schwartz H, Blacher E, Amer M, Livneh N, Abramovitz L, Klein A, et al. Incipient Melanoma Brain Metastases Instigate Astrogliosis and Neuroinflammation. Cancer Res. 2016; 76: 4359-71.

68. Valiente M, Van Swearingen AED, Anders CK, Bairoch A, Boire A, Bos PD, et al. Brain Metastasis Cell Lines Panel: A Public Resource of Organotropic Cell Lines. Cancer Res. 2020; 80: 4314-23.
69. Zhang Z, Hatori T, Nonaka H. An experimental model of brain metastasis of lung carcinoma. Neuropathology. 2008; 28: 24-8.
70. Choi MR, Bardhan R, Stanton-Maxey KJ, Badve S, Nakshatri H, Stantz KM, et al. Delivery of nanoparticles to brain metastases of breast cancer using a cellular Trojan horse. Cancer Nanotechnol. 2012; 3: 47-54.
71. Peng L, Wang Y, Fei S, Wei C, Tong F, Wu G, et al. The effect of combining Endostar with radiotherapy on blood vessels, tumor-associated macrophages, and T cells in brain metastases of Lewis lung cancer. Transl Lung Cancer Res. 2020; 9: 745-60.
72. Nakahara N, Okada H, Witham TF, Attanucci J, Fellows WK, Chambers WH, et al. Combination of stereotactic radiosurgery and cytokine gene-transduced tumor cell vaccination: a new strategy against metastatic brain tumors. J Neurosurg. 2001; 95: 984-9.
73. Wu CC, Chaudhary KR, Na YH, Welch D, Black PJ, Sonabend AM, et al. Quality Assessment of Stereotactic Radiosurgery of a Melanoma Brain Metastases Model Using a Mouselike Phantom and the Small Animal Radiation Research Platform. Int J Radiat Oncol Biol Phys. 2017; 99: 191-201.
74. Li X, Wang Y, Wang J, Zhang T, Zheng L, Yang Z, et al. Enhanced efficacy of AZD3759 and radiation on brain metastasis from EGFR mutant non-small cell lung cancer. Int J Cancer. 2018; 143: 212-24.
75. Choi SH, Yang H, Lee SH, Ki JH, Nam DH, Yoo HY. TopBP1 and Claspin contribute to the radioresistance of lung cancer brain metastases. Mol Cancer. 2014; 13: 211.
76. Smart D, Garcia-Glaessner A, Palmieri D, Wong-Goodrich SJ, Kramp T, Gril B, et al. Analysis of radiation therapy in a model of triple-negative breast cancer brain metastasis. Clin Exp Metastasis. 2015; 32: 717-27.
77. Remsen LG, Marquez C, Garcia R, Thrun LA, Neuwelt EA. Efficacy after sequencing of brain radiotherapy and enhanced antibody targeted chemotherapy delivery in a rodent human lung cancer brain xenograft model. Int J Radiat Oncol Biol Phys. 2001; 51: 1045-9.
78. Murrell DH, Zarghami N, Jensen MD, Dickson F, Chambers AF, Wong E, et al. MRI surveillance of cancer cell fate in a brain metastasis model after early radiotherapy. Magn Reson Med. 2017; 78: 1506-12.
79. Zarghami N, Murrell DH, Jensen MD, Dick FA, Chambers AF, Foster PJ, et al. Half brain irradiation in a murine model of breast cancer brain metastasis: magnetic resonance imaging and histological assessments of dose-response. Radiat Oncol. 2018; 13: 104.
80. Fowler JF. 21 years of biologically effective dose. Br J Radiol. 2010; 83: 554-68.
81. Kirkpatrick JP, Meyer JJ, Marks LB. The linear-quadratic model is inappropriate to model high dose per fraction effects in radiosurgery. Semin Radiat Oncol. 2008; 18: 240-3.
82. Wall BA, Yu LJ, Khan A, Haffty B, Goydos JS, Chen S. Riluzole is a radio-sensitizing agent in an *in vivo* model of brain metastasis derived from GRM1 expressing human melanoma cells. Pigment Cell Melanoma Res. 2015; 28: 105-9.
83. Tsao MN, Xu W, Wong RK, Lloyd N, Laperriere N, Sahgal A, et al. Whole brain radiotherapy for the treatment of newly diagnosed multiple brain metastases. Cochrane Database Syst Rev. 2018; 1: Cd003869.
84. Nabors LB, Portnow J, Ahluwalia M, Baehring J, Brem H, Brem S, et al. Central Nervous System Cancers, Version 3.2020, NCCN Clinical Practice Guidelines in Oncology. J Natl Compr Canc Netw. 2020; 18: 1537-70.
85. Bobyk L, Edouard M, Deman P, Vautrin M, Pernet-Gallay K, Delaroche J, et al. Photoactivation of gold nanoparticles for glioma treatment. Nanomedicine. 2013; 9: 1089-97.
86. Delaney LJ, Ciraku L, Oeffinger BE, Wessner CE, Liu JB, Li J, et al. Breast Cancer Brain Metastasis Response to Radiation After Microbubble Oxygen Delivery in a Murine Model. J Ultrasound Med. 2019; 38: 3221-8.
87. Corroyer-Dulmont A, Valable S, Falzone N, Frelin-Labalme AM, Tietz O, Toutain J, et al. VCAM-1 targeted alpha-particle therapy for early brain metastases. Neuro Oncol. 2020; 22: 357-68.
88. Monteiro C, Miarka L, Perea-García M, Priego N, García-Gómez P, Álvaro-Espinosa L, et al. Stratification of radiosensitive brain metastases based on an actionable S100A9/RAGE resistance mechanism. Nat Med. 2022; 28: 752-65.
89. Liu JL, Tian DS, Li ZW, Qu WS, Zhan Y, Xie MJ, et al. Tamoxifen alleviates irradiation-induced brain injury by attenuating microglial inflammatory response *in vitro* and *in vivo*. Brain Res. 2010; 1316: 101-11.
90. Son Y, Yang M, Wang H, Moon C. Hippocampal dysfunctions caused by cranial irradiation: a review of the experimental evidence. Brain Behav Immun. 2015; 45: 287-96.
91. van Leeuwen CM, Oei AL, Crezee J, Bel A, Franken NAP, Stalpers LJA, et al. The alfa and beta of tumours: a review of parameters of the linear-quadratic model, derived from clinical radiotherapy studies. Radiat Oncol. 2018; 13: 96.
92. Garcia LM, Leblanc J, Wilkins D, Raaphorst GP. Fitting the linear-quadratic model to detailed data sets for different dose ranges. Phys Med Biol. 2006; 51: 2813-23.
93. Duregon E, Senetta R, Pittaro A, Verdun di Cantogno L, Stella G, De Blasi P, et al. CAVEOLIN-1 expression in brain metastasis from lung cancer predicts worse outcome and radioresistance, irrespective of tumor histotype. Oncotarget. 2015; 6: 29626-36.
94. Steeg PS. The blood-tumour barrier in cancer biology and therapy. Nat Rev Clin Oncol. 2021; 18: 696-714.
95. Khatri A, Gaber MW, Brundage RC, Naimark MD, Hanna SK, Stewart CF, et al. Effect of radiation on the penetration of irinotecan in rat cerebrospinal fluid. Cancer Chemother Pharmacol. 2011; 68: 721-31.
96. Zeng YD, Liao H, Qin T, Zhang L, Wei WD, Liang JZ, et al. Blood-brain barrier permeability of gefitinib in patients with brain metastases from non-small-cell lung cancer before and during whole brain radiation therapy. Oncotarget. 2015; 6: 8366-76.
97. Teng F, Tsien CI, Lawrence TS, Cao Y. Blood-tumor barrier opening changes in brain metastases from pre to one-month post radiation therapy. Radiother Oncol. 2017; 125: 89-93.
98. Mahmoud-Ahmed AS, Suh JH, Barnett GH, Webster KD, Belinson JL, Kennedy AW. The effect of radiation therapy on brain metastases from endometrial carcinoma: a retrospective study. Gynecol Oncol. 2001; 83: 305-9.
99. Wang S, Wu CC, Zhang H, Karakatsani ME, Wang YF, Han Y, et al. Focused ultrasound induced-blood-brain barrier opening in mouse brain receiving radiosurgery dose of radiation enhances local delivery of systemic therapy. Br J Radiol. 2020; 93: 20190214.
100. Blethen KE, Sprowls SA, Arsiwala TA, Wolford CP, Panchal DM, Fladeland RA, et al. Effects of whole-brain radiation therapy on the blood-brain barrier in immunocompetent and immunocompromised mouse models. Radiat Oncol. 2023; 18: 22.
101. Takahashi J, Nagasawa S, Ikemoto MJ, Sato C, Sato M, Iwahashi H. Verification of 5-Aminolevurinic Radiodynamic Therapy Using a Murine Melanoma Brain Metastasis Model. Int J Mol Sci. 2019; 20.
102. Kil WJ, Cerna D, Burgan WE, Beam K, Carter D, Steeg PS, et al. *In vitro* and *in vivo* radiosensitization induced by the DNA methylating agent temozolomide. Clin Cancer Res. 2008; 14: 931-8.
103. Lee SY. Temozolomide resistance in glioblastoma multiforme. Genes Dis. 2016; 3: 198-210.
104. Huang RX, Zhou PK. DNA damage response signaling pathways and targets for radiotherapy sensitization in cancer. Signal Transduct Target Ther. 2020; 5: 60.
105. Pomeranz Krummel DA, Nasti TH, Izar B, Press RH, Xu M, Lowder L, et al. Impact of Sequencing Radiation Therapy and Immune Checkpoint Inhibitors in the Treatment of Melanoma Brain Metastases. Int J Radiat Oncol Biol Phys. 2020; 108: 157-63.
106. Yang Y, Deng L, Yang Y, Zhang T, Wu Y, Wang L, et al. Efficacy and Safety of Combined Brain Radiotherapy and Immunotherapy in Non-Small-Cell Lung Cancer With Brain Metastases: A Systematic Review and Meta-Analysis. Clin Lung Cancer. 2022; 23: 95-107.
107. Buchwald ZS, Wynne J, Nasti TH, Zhu S, Mourad WF, Yan W, et al. Radiation, Immune Checkpoint Blockade and the Abscopal Effect: A Critical Review on Timing, Dose and Fractionation. Front Oncol. 2018; 8: 612.
108. Montay-Gruel P, Acharya MM, Gonçalves Jorge P, Petit B, Petridis IG, Fuchs P, et al. Hypofractionated FLASH-RT as an Effective Treatment against Glioblastoma that Reduces Neurocognitive Side Effects in Mice. Clin Cancer Res. 2021; 27: 775-84.
109. Chang S, Liu G, Zhao L, Zheng W, Yan D, Chen P, et al. Redefine the Role of Spot-Scanning Proton Beam Therapy for the Single Brain Metastasis Stereotactic Radiosurgery. Front Oncol. 2022; 12: 804036.
110. Marullo R, Castro M, Yomtoubian S, Calvo-Vidal MN, Revuelta MV, Krumsiek J, et al. The metabolic adaptation evoked by arginine enhances the effect of radiation in brain metastases. Sci Adv. 2021; 7: eabg1964.
111. Sharma S, Wu SY, Jimenez H, Xing F, Zhu D, Liu Y, et al. Ca(2+) and CACNA1H mediate targeted suppression of breast cancer brain metastasis by AM RF EMF. EBioMedicine. 2019; 44: 194-208.
112. Larkin JR, Simard MA, de Bernardi A, Johanssen VA, Perez-Balderas F, Sibson NR. Improving Delineation of True Tumor Volume With Multimodal MRI in a Rat Model of Brain Metastasis. Int J Radiat Oncol Biol Phys. 2020; 106: 1028-38.
113. Potez M, Bouchet A, Flaender M, Rome C, Collomb N, Grotzer M, et al. Synchrotron X-Ray Boost Delivered by Microbeam Radiation Therapy After Conventional X-Ray Therapy Fractionated in Time Improves F98 Glioma Control. Int J Radiat Oncol Biol Phys. 2020; 107: 360-9.
114. Lonser RR, Walbridge S, Vortmeyer AO, Pack SD, Nguyen TT, Gogate N, et al. Induction of glioblastoma multiforme in nonhuman primates after therapeutic doses of fractionated whole-brain radiation therapy. J Neurosurg. 2002; 97: 1378-89.
115. Krisht AF, Yoo K, Arnautovic KI, Al-Mefty O. Cavernous sinus tumor model in the canine: a simulation model for cavernous sinus tumor surgery. Neurosurgery. 2005; 56: 1361-5; discussion 5-6.
116. Zheng L, Sun P, Zheng S, Han Y, Zhang G. Functional dynamic contrast-enhanced magnetic resonance imaging in an animal model of brain metastases: a pilot study. PLoS One. 2014; 9: e109308.
117. Williams KC, Cepeda MA, Javed S, Searle K, Parkins KM, Makela AV, et al. Invadopodia are chemosensing protrusions that guide cancer cell extravasation to promote brain tropism in metastasis. Oncogene. 2019; 38: 3598-615.
118. Javed S, Soukhtehzari S, Salmond N, Fernandes N, Williams KC. Development of an *in vivo* system to model breast cancer metastatic organotropism and evaluate treatment response using the chick embryo. iScience. 2023; 26: 106305.
119. Power EA, Fernandez-Torres J, Zhang L, Yaun R, Lucien F, Daniels DJ. Chorioallantoic membrane (CAM) assay to study treatment effects in diffuse intrinsic pontine glioma. PLoS One. 2022; 17: e0263822.

120. Li J, Huang D, Lei B, Huang J, Yang L, Nie M, et al. VLA-4 suppression by senescence signals regulates meningeal immunity and leptomeningeal metastasis. NA. 2022; 11.
121. Chi Y, Remsik J, Kiseliovas V, Derderian C, Sener U, Alghader M, et al. Cancer cells deploy lipocalin-2 to collect limiting iron in leptomeningeal metastasis. Science. 2020; 369: 276-82.
122. Svendsen HA, Meling TR, Nygaard V, Waagene S, Russnes H, Juell S, et al. Novel human melanoma brain metastasis models in athymic nude fox1(nu) mice: Site-specific metastasis patterns reflecting their clinical origin. Cancer Med. 2021; 10: 8604-13.
123. Xu M, Wang Y, Duan W, Xia S, Wei S, Liu W, et al. Proteomic Reveals Reasons for Acquired Drug Resistance in Lung Cancer Derived Brain Metastasis Based on a Newly Established Multi-Organ Microfluidic Chip Model. Front Bioeng Biotechnol. 2020; 8: 612091.
124. Xu Z, Li E, Guo Z, Yu R, Hao H, Xu Y, et al. Design and Construction of a Multi-Organ Microfluidic Chip Mimicking the *in vivo* Microenvironment of Lung Cancer Metastasis. ACS Appl Mater Interfaces. 2016; 8: 25840-7.
125. Krieger TG, Tirier SM, Park J, Jechow K, Eisemann T, Peterziel H, et al. Modeling glioblastoma invasion using human brain organoids and single-cell transcriptomics. Neuro Oncol. 2020; 22: 1138-49.
126. Sheu T, Molkentine J, Transtrum MK, Buchholz TA, Withers HR, Thames HD, et al. Use of the LQ model with large fraction sizes results in underestimation of isoeffect doses. Radiother Oncol. 2013; 109: 21-5.
127. Contreras-Zárate MJ, Alvarez-Eraso KLF, Jaramillo-Gómez JA, Littrell Z, Tsuji N, Ormond DR, et al. Short-term topiramate treatment prevents radiation-induced cytotoxic edema in preclinical models of breast-cancer brain metastasis. Neuro Oncol. 2023.
128. Hartmann J, Wölfelschneider J, Stache C, Buslei R, Derer A, Schwarz M, et al. Novel technique for high-precision stereotactic irradiation of mouse brains. Strahlenther Onkol. 2016; 192: 806-14.
129. Wong J, Armour E, Kazanzides P, Iordachita I, Tryggestad E, Deng H, et al. High-resolution, small animal radiation research platform with x-ray tomographic guidance capabilities. Int J Radiat Oncol Biol Phys. 2008; 71: 1591-9.
130. Park I, Kim S, Pucciarelli D, Song J, Choi JM, Lee KH, et al. Differentiating Radiation Necrosis from Brain Tumor Using Hyperpolarized Carbon-13 MR Metabolic Imaging. Mol Imaging Biol. 2021; 23: 417-26.
131. Clarkson R, Lindsay PE, Ansell S, Wilson G, Jelveh S, Hill RP, et al. Characterization of image quality and image-guidance performance of a preclinical microirradiator. Med Phys. 2011; 38: 845-56.
132. Tillner F, Hietschold V, Khaless A, Pawelke J, Thute P, Enghardt W. Characterization and optimization of the imaging and dosimetric properties of a image-guided precision irradiation device for small animals. Strahlentherapie Und Onkologie. 2010; 186: 105-.
133. Silginer M, Weller M, Stupp R, Roth P. Biological activity of tumor-treating fields in preclinical glioma models. Cell Death Dis. 2017; 8: e2753.
134. Jin Y, Kang Y, Peng X, Yang L, Li Q, Mei Q, et al. Irradiation-Induced Activated Microglia Affect Brain Metastatic Colonization of NSCLC Cells via miR-9/CDH1 Axis. Onco Targets Ther. 2021; 14: 1911-22.